Partial Differential Equations in Applied Mathematics 12 (2024) 101001

Contents lists available at ScienceDirect

Partial Differential Equations in Applied Mathematics

journal homepage: www.elsevier.com/locate/padiff

Analytical solutions to the (2+1)-dimensional cubic Klein–Gordon equation in the presence of fractional derivatives: A comparative study

K. M. Abdul Al Woadud [a,b,*], Md. Jahirul Islam [b], Dipankar Kumar [c], Aminur Rahman Khan [a]

[a] Department of Mathematics, Jahangirnagar University, Savar, Dhaka 1342, Bangladesh
[b] Department of Mathematics, Uttara University, Dhaka 1230, Bangladesh
[c] Department of Mathematics, Bangabandhu Sheikh Mujibur Rahman Science and Technology University, Gopalganj 8100, Bangladesh

ARTICLE INFO

Keywords:
Cubic Klein–Gordon equation
Beta derivative
The unified method
Wave propagation

ABSTRACT

The study seeks to obtain new analytical solutions for the (2+1)-dimensional cubic Klein–Gordon (cKG) equation using the beta derivative. By applying the unified method to the equation, various types of solitons have been generated, including periodic solitons, periodic solitons with equal and unequal wavelengths, bright solitons, and periodic singular solitons with unequal wavelengths. To demonstrate the fundamental dynamics of the soliton family, three-dimensional and two-dimensional graphs showcasing various novel solutions that satisfy the relevant equations are provided. In relation to fractionality, the bright waveform retains its overall shape, but its smoothness improves as the fractional parameters increase. Conversely, periodic wave solutions show enhanced periodicity as the fractional parameters rise. Additionally, the study provides a comprehensive comparison of solutions derived from models utilizing conformable, M-truncated, and beta derivatives. The investigation explores the effect of the fractional parameter on soliton amplitude, using graphs to illustrate this impact by assigning specific values to the fractional parameter. The properties of the waves can be modified through changes to the model's parameters to produce the appropriate wave profiles. Consequently, the solutions we obtained could be particularly valuable for analyzing physical problems associated with nonlinear complex dynamical systems.

Introduction

Background and motivation

Nonlinear evolution equations (NLEEs) appear in many scientific applications such as beam propagation, particle physics, fluid mechanics, marine engineering, nonlinear optics, elasticity theory, solid-state physics, and quantum field theory, and provide a crucial part for the modeling of real-world problems. The well-known nonlinear Klein–Gordon equation continues to attract significant interest from many researchers working in this field. The Klein–Gordon equation, proposed by Oskar Klein and Walter Gordon in 1926. The cubic Klein–Gordon equation is used model many different nonlinear phenomena, including the propagation of dislocation in crystals and the behavior of elementary particles and the propagation of fluxions in Josephson junctions. This equation is a relativistic field equation for scalar particles and is a relativistic generalization of the well-known Schrödinger equation.[1,2] It has numerous applications in physics and engineering, such as quantum field theory, relativistic physics, dispersive wave phenomena, plasma physics, and nonlinear optics. Analytical solutions are gradually becoming more significant in numerous applied scientific and engineering areas. The exact solution plays an important role in evaluating nonlinear phenomena that have happened in many areas of nonlinear science, including particle physics. One of the most important objectives of nonlinear science and engineering is to find exact solutions to NLEEs using analytical methods. Many scholars are keen to solve the NLEEs using significant methods of analysis, for example the homogeneous balance method,[3] the modified simple equation method,[4] the extended tanh function method,[5] the extended F-expansion method,[6] the(G'/G)-expansion method,[7] the generalized Kudryashov method,[8] the Weierstrass elliptic function expansion method,[9] the transformed rational function method,[10] the Weierstrass elliptic function expansion method,[11] the modified Kudryashov method,[12–17] the sine-Gordon equation expansion method,[18,19] the extended sinh-Gordon equation method,[20–22] the hyperbolic function method,[23] the generalised exponential rational function method and the

* Corresponding author at: Department of Mathematics, Jahangirnagar University, Savar, Dhaka 1342, Bangladesh.
E-mail address: woadudru50@gmail.com (K.M.A.A. Woadud).

https://doi.org/10.1016/j.padiff.2024.101001
Received 11 September 2024; Received in revised form 22 October 2024; Accepted 17 November 2024
Available online 19 November 2024

Kudryashov's simplest equation method,[24] the generalised Riccati mapping method,[25] the GERF method,[26] the lie symmetry method,[27–34] the modified generalized exponential rational function method.[35,36] In this sense, we verified our recently found solutions by back substituting the related PDE using the Maple 18 software, and the results showed that they were accurate.

Governing model and litarature review

We consider the (2+1) dimensional cubic Klein–Gordon equation is given by

$$V_{xx} + V_{yy} - V_{tt} + \alpha V + \beta V^3 = 0, \tag{1}$$

Where $V = V(x, y, t)$ and α, β are non zero constants.

Eq. (1) produces cubic Klein–Gordon equation. Numerous investigations into the models have been carried out (1). For instance, Kaur et al.[37] discovered kink and periodic soliton solutions of the cKG equation using the assistance of the modified exponential expansion method. The modified simple equation method is used for cKG equations.[38] The modified simple equation method produces singular kink, kink, singular periodic and periodic soliton solutions. Asaduzzaman and Kilicman[39] construct some uniform a priori estimates of approximate solution to the corresponding equation using Galerkin's method. First integral method is used to acquire the analytical solutions of cKG equation such as cuspon and periodic solution.[40] The modified extended mapping method is used to acquire the analytical solutions of cKG equation such as bright, kink, anti-kink, periodic solution.[41] According to the literature,[37–41] analytical solutions for the (2+1)-dimensional cKG equation with the beta derivative have not yet been found in any study. Some authors have already used the unified method to solve a number of nonlinear PDEs involving fractional calculus. In the current study, the studied equation will be solved using the unified method in the presence of the beta derivative. According to Refs.,[42,43] the unified method is unique and effective since it removes the limitations and scarcity of current methods, for example (i) the tanh-function method,[44] (ii) the extended tanh-function method,[45] (iii) the modified extended tanh function method,[46] (iv) the complex tanh-function method,[47] (v) the G'/G-expansion method,[48] (vi) the generalized G'/G-expansion method,[49] and (vii) the $(G'/G, 1/G)$-expansion method.[50,51] Benefits of the unified method, (i), it produces a lot of solutions than other methods. (ii), it combines all of the methods' advantages into a single method without needing additional work. In contrast, it minimizes the amount of work done on the computer to the point where it is occasionally even done by hand.

Beta derivative and method's outline

Introduction of fractional derivative

Fractional calculus is an extension of classical calculus that generalizes its concepts. It has several applications in various fields of mathematics, physics, and engineering. The most effective way to achieve this is with fractional partial differential equations (FPDEs), which are used in engineering and physical processes. These equations have gained in importance and popularity in recent years due to their potential applications in mathematical physics, biology, and nonlinear optics. The definitions of fractional derivatives (FDs) have been widely circulated in the literature in recent years in order to highlight recent developments in the field of fractional calculus and its practical applications in many research fields, such as the Caputo derivative, Grünwald–Letnikov derivative, modified Riemann-Liouville derivative, Local fractional derivative, Conformable derivative, M-truncated derivative, Atangana-Baleanu derivative, Atangana-Baleanu-Riemann derivative, Atangana's conformable derivative, etc. (Refs.[52–61]). Tarasov[62] stated that the generalized Leibniz rule must be followed by a fractional operator. According to this explanation, fractional derivatives with non-integer orders, such as the Jumarie derivative and the local derivative, are fundamentally unable to matching the Leibniz rule's conditions. In addition, within the framework of a real-world application, Cresson and Szafranska[63] went into great detail about a number of topics related to Jumarie's fractional derivative and the local fractional derivative. The definition and properties of Atangana's derivative, also known as the beta derivative, are the main topics of this research because it might be challenging to determine the accurate fractional derivatives. A thorough explanation of the several FD definitions, behaviors, and restrictions can be found in Ref.[64] We will look at the definition and a key property of Atangana's conformable derivative or the beta derivative. Atangana et al.[60] were the first to introduce the concept of the beta derivative and to explore its properties. Later, Atangana and Alqahtani[61] demonstrated that the beta-derivative can more precisely explain the spread of the river blindness disease model than the Caputo derivative.

Atangana et al.[60] provided the following definition of ACD based only on the fundamental limit definition of the derivative:

$${}_0^A D_t^{\tau}(f(t)) = \lim_{\Delta h \to 0} \frac{f\left(t + \Delta h\left(t + \frac{1}{\Gamma(\tau)}\right)^{1-\tau}\right) - f(t)}{\Delta h}, \text{ for all } t > 0,\ 0 < \tau \le 1.$$

This derivative is also referred to as the beta derivative. For a better understanding, let us study some of the useful aspects of the beta derivative as per Ref.[54] The definition and properties of the beta derivative will be utilized in this study.

Considering that, $p, q \in \mathbb{R}$**,** where $\mathbb{R}$ is the set of all real numbers, $g = g(t) \neq 0$ and $f = f(t)$ are two functions τ-differentiable at a point $t > 0$, whereas $\tau \in (0, 1]$, we have

(i). ${}_0^A D_t^{\tau}(pf(t) + qg(t)) = p{}_0^A D_t^{\tau} f(t) + q{}_0^A D_t^{\tau} g(t),\ \forall\, p, q \in \mathbb{R}.$

(ii). ${}_0^A D_t^{\tau}(C) = 0$, where C is a constant.

(iii). ${}_0^A D_t^{\tau}(f(t)g(t)) = g(t)\, {}_0^A D_t^{\tau} f(t) + f(t){}_0^A D_t^{\tau} g(t).$

(iv). ${}_0^A D_x^{\tau}\left(\frac{f(t)}{g(t)}\right) = \frac{g(t){}_0^A D_x^{\tau} f(t) - f(t){}_0^A D_t^{\tau} g(t)}{(g(t))^2}.$

By considering $\Delta h = \left(t + \frac{1}{\Gamma\tau}\right)^{\tau-1} h,\ h \to 0$ when $\Delta h \to 0$. As a result, we get the following desirable property: ${}_0^A D_t^{\tau} f(t) = \left(t + \frac{1}{\Gamma\tau}\right)^{1-\tau} \frac{df(t)}{dt}.$

Overviews of the unified method

Let us consider the general form of the NLEEs as:

$$P\left(V,\ {}_0^A D_x^{\tau} V,\ {}_0^A D_y^{\tau} V,\ {}_0^A D_t^{\tau} V,\ {}_0^A D_{xx}^{2\tau} V,\ {}_0^A D_{yy}^{2\tau} V,\ {}_0^A D_{tt}^{2\tau} V \cdots\cdots\cdots\right) = 0 \tag{2}$$

where $V(x, y, t)$ is an unknown function, P is a polynomial of $V = V(x, y, t)$.

The introduction of the transformation using the beta derivative

$$V(x, y, t; \tau) = v(\xi),\ \xi = \frac{1}{\tau}\left(\left(x + \frac{1}{\Gamma\tau}\right)^{\tau} + \left(y + \frac{1}{\Gamma\tau}\right)^{\tau} - \lambda\left(t + \frac{1}{\Gamma\tau}\right)^{\tau}\right) \tag{3}$$

Eq. (2) is converted into the following ordinary differential equation (ODE):

$$Q(v, vv', v',\ v'' \cdots\cdots\cdots) = 0, \tag{4}$$

Here, the superscripts indicate the ordinary derivatives with respect to ξ, Q is a polynomial of v and its derivatives.

According to the unified method, the exact soliton solution of Eq. (4) is conjecture to be

$$v(\xi) = a_0 + \sum_{i=1}^{N} \left(a_i\varphi^i + b_i\varphi^{-i}\right), \tag{5}$$

where $\phi = \phi(\xi)$ satisfies the Riccati differential equation

$$\varphi'(\xi) = \varphi^2(\xi) + B \tag{6}$$

where $\varphi' = \frac{d\varphi}{d\xi}$, and a_i, b_i, and B are constants. The general solutions of Eq. (6) are as follows:

Cluster 1: If $B < 0$, then the hyperbolic function solutions are

$$\varphi(\xi) = \begin{cases} \dfrac{\sqrt{-(G^2+H^2)B} - G\sqrt{-B}\,cosh\left(2\sqrt{-B}\,(\xi+F)\right)}{G\sinh\left(2\sqrt{-B}\,(\xi+F)\right)+H} \\ \dfrac{-\sqrt{-(G^2+H^2)B} - G\sqrt{-B}\,cosh\left(2\sqrt{-B}\,(\xi+F)\right)}{G\sinh\left(2\sqrt{-B}\,(\xi+F)\right)+H} \\ \sqrt{-B} - \dfrac{2G\sqrt{-B}}{G+cosh\left(2\sqrt{-B}\,(\xi+F)\right)-sinh\left(2\sqrt{-B}\,(\xi+F)\right)} \\ -\sqrt{-B} + \dfrac{2G\sqrt{-B}}{G+cosh\left(2\sqrt{-B}\,(\xi+F)\right)+sinh\left(2\sqrt{-B}\,(\xi+F)\right)} \end{cases}, \tag{7}$$

Cluster 2: If $B > 0$, then the trigonometric function solutions are

$$\varphi(\xi) = \begin{cases} \dfrac{\sqrt{(G^2-H^2)B} - G\sqrt{B}\,cos\left(2\sqrt{B}\,(\xi+F)\right)}{G\sin\left(2\sqrt{B}\,(\xi+F)\right)+H} \\ \dfrac{-\sqrt{(G^2-H^2)B} - G\sqrt{B}\,cos\left(2\sqrt{B}\,(\xi+F)\right)}{G\sin\left(2\sqrt{B}\,(\xi+F)\right)+H} \\ i\sqrt{B} - \dfrac{2Gi\sqrt{B}}{G+cos\left(2\sqrt{B}\,(\xi+F)\right)-isin\left(2\sqrt{B}\,(\xi+F)\right)} \\ -i\sqrt{B} + \dfrac{2Gi\sqrt{B}}{G+cos\left(2\sqrt{B}\,(\xi+F)\right)+isin\left(2\sqrt{B}\,(\xi+F)\right)} \end{cases}, \tag{8}$$

Cluster 3: If $B = 0$, then the rational function solution is

$$\varphi(\xi) = -\frac{1}{\xi+F}, \tag{9}$$

where G, H, and F are three real arbitrary constants.

We get the values of N by using the balance procedure in Eq. (4). Furthermore, the degree of $v(\xi)$ is $D[v(\xi)] = N$, resulting in the following order of expression: $D\left[\frac{d^q v}{d\xi^q}\right] = N + q$, $D\left[v^r\left(\frac{d^q v}{d\xi^q}\right)^s\right] = Nr + s(q+N)$. Thus, the value of N in Eq. (5) is found.

Eq. (5) insert to Eq. (4) and use Eq. (6), then subtract all terms like $\varphi(\xi)$, then assign each product to an over-defined system of algebraic equations, and then solve the system of algebraic equations a_i, b_i, λ and B. We have several sets of solutions.

Finally, substituting a_i, b_i, λ and B into Eq. (5) and using the trail solutions of Eq. (6), explicit solutions of Eq. (2) can be obtained immediately depending on the value B.

Mathematical analysis

We consider the (2+1) dimensional cubic Klein–Gordon equation with beta derivative

$${}_0^A D_{xx}^{2\tau} V + {}_0^A D_{yy}^{2\tau} V - {}_0^A D_{tt}^{2\tau} V + \alpha V + \beta V^3 = 0 \tag{10}$$

Where ${}_0^A D_{xx}^{2\tau} V$, ${}_0^A D_{yy}^{2\tau} V$ and ${}_0^A D_{tt}^{2\tau} V$ represent the beta derivative with order τ with respect to t, x, y, and $0 < \tau < 1$. By substituting $\tau = 1$, the fractional-order cKG equation in Eq. (10) transforms into the integer-order cKG equation. Assume the following transformation the (2+1)-dimensional cKG equation with beta derivative:

$$V(x, y, t; \tau) = v(\xi),\ \xi = \frac{1}{\tau}\left(\left(x+\frac{1}{\Gamma\tau}\right)^{\tau} + \left(y+\frac{1}{\Gamma\tau}\right)^{\tau} - \lambda\left(t+\frac{1}{\Gamma\tau}\right)^{\tau}\right) \tag{11}$$

Using Eq. (11) into the (2+1) dimensional cubic Klein–Gordon Eq. (1), which can be reduced to a nonlinear ordinary differential equation as shown below

$$\left(2-\lambda^2\right)v'' + \alpha v + \beta v^3 = 0 \tag{12}$$

N=1 is found using the homogeneous balancing principle. The answer to Eq. (12) then takes the form

$$v(\xi) = A_0 + A_1(\varphi(\xi)) + B_1(\varphi(\xi))^{-1}. \tag{13}$$

By substituting Eq. (12) into Eq. (11) and equating the like powers of $\varphi(\xi)$, a system of equations is obtained. After solving, the following solution sets are obtained:

Set 1: $A_0 = 0$, $A_1 = 0$, $B_1 = \pm\frac{\sqrt{\beta B\alpha}}{\beta}$, and $\lambda = \frac{1}{2}\,\frac{\sqrt{2}\,\sqrt{B(4B+\alpha)}}{B}$

Set 2: $A_0 = 0$, $A_1 = 0$, $B_1 = \pm\frac{\sqrt{\beta B\alpha}}{\beta}$, and $\lambda = -\frac{1}{2}\,\frac{\sqrt{2}\,\sqrt{B(4B+\alpha)}}{B}$

Set 3: $A_0 = 0$, $A_1 = \pm\frac{\sqrt{\beta B\alpha}}{B\beta}$, $B_1 = 0$, and $\lambda = \frac{1}{2}\,\frac{\sqrt{2}\,\sqrt{B(4B+\alpha)}}{B}$

Set 4: $A_0 = 0$, $A_1 = \pm\frac{\sqrt{\beta B\alpha}}{B\beta}$, $B_1 = 0$, and $\lambda = -\frac{1}{2}\,\frac{\sqrt{2}\,\sqrt{B(4B+\alpha)}}{B}$

Set 5: $A_0 = 0$, $A_1 = \pm\frac{1}{2}\,\frac{\sqrt{-2\beta B\alpha}}{B\beta}$, $B_1 = \mp\frac{\alpha\beta}{\sqrt{-2\beta B\alpha}}$, and $\lambda = \frac{1}{2}\,\frac{\sqrt{(8B-\alpha)B}}{B}$

Set 6: $A_0 = 0$, $A_1 = \pm\frac{1}{2}\,\frac{\sqrt{-2\beta B\alpha}}{B\beta}$, $B_1 = \mp\frac{\alpha\beta}{\sqrt{-2\beta B\alpha}}$, and $\lambda = -\frac{1}{2}\,\frac{\sqrt{(8B-\alpha)B}}{B}$

Set 7: $A_0 = 0$, $A_1 = \pm\frac{1}{2}\,\frac{\sqrt{\beta B\alpha}}{B\beta}$, $B_1 = \mp\frac{1}{2}\,\frac{\alpha\beta}{\sqrt{\beta B\alpha}}$, and $\lambda = \frac{1}{4}\,\frac{\sqrt{2}\,\sqrt{(16B+\alpha)B}}{B}$

Set 8: $A_0 = 0$, $A_1 = \pm\frac{1}{2}\,\frac{\sqrt{\beta B\alpha}}{B\beta}$, $B_1 = \mp\frac{1}{2}\,\frac{\alpha\beta}{\sqrt{\beta B\alpha}}$, and $\lambda = -\frac{1}{4}\,\frac{\sqrt{2}\,\sqrt{(16B+\alpha)B}}{B}$

Set 1 this corresponds to the solutions of the analyzed model obtained through the application of Eqs. (7)–(11):

$$V_{1,2}(x,y,t) = \pm\frac{\sqrt{\beta B\alpha}}{\beta}\left(\frac{\sqrt{-(G^2+H^2)B} - G\sqrt{-B}\,cosh\left(2\sqrt{-B}(\xi+F)\right)}{G\sinh\left(2\sqrt{-B}(\xi+F)\right)+H}\right)^{-1}, \tag{14}$$

$$V_{3,4}(x,y,t) = \pm\frac{\sqrt{\beta B\alpha}}{\beta}\left(\frac{-\sqrt{-(G^2+H^2)B} - G\sqrt{-B}\,cosh\left(2\sqrt{-B}(\xi+F)\right)}{G\sinh\left(2\sqrt{-B}(\xi+F)\right)+H}\right)^{-1}, \tag{15}$$

$$V_{5,6}(x,\ y,\ t) = \pm\frac{\sqrt{\beta B\alpha}}{\beta}\left(\sqrt{-B} - \frac{2G\sqrt{-B}}{G+cosh\left(2\sqrt{-B}\,(\xi+F)\right) - sinh\left(2\sqrt{-B}\,(\xi+F)\right)}\right)^{-1}, \tag{16}$$

$$V_{7,8}(x,\ y,\ t) = \pm\frac{\sqrt{\beta B\alpha}}{\beta}\left(-\sqrt{-B} + \frac{2G\sqrt{-B}}{G+cosh\left(2\sqrt{-B}\,(\xi+F)\right) + sinh\left(2\sqrt{-B}\,(\xi+F)\right)}\right)^{-1}, \tag{17}$$

$$V_{9,10}(x,\ y,\ t) = \pm\frac{\sqrt{\beta B\alpha}}{\beta}\left(\frac{\sqrt{(G^2-H^2)B} - G\sqrt{B}\ cos\left(2\sqrt{B}\,(\xi+F)\right)}{G\sin\left(2\sqrt{B}\,(\xi+F)\right)+H}\right)^{-1}, \tag{18}$$

$$V_{11,12}(x,y,t) = \pm\frac{\sqrt{\beta B\alpha}}{\beta}\left(\frac{-\sqrt{(G^2-H^2)B} - G\sqrt{B}\,cos\left(2\sqrt{B}\,(\xi+F)\right)}{G\sin\left(2\sqrt{B}\,(\xi+F)\right)+H}\right)^{-1}, \tag{19}$$

$$V_{13,14}(x,\ y,\ t) = \pm\frac{\sqrt{\beta B\alpha}}{\beta}\left(i\sqrt{B} - \frac{2Gi\sqrt{B}}{G+cos\left(2\sqrt{B}\,(\xi+F)\right) - isin\left(2\sqrt{B}\,(\xi+F)\right)}\right)^{-1}, \tag{20}$$

$$V_{15,16}(x,\ y,\ t) = \pm\frac{\sqrt{\beta B\alpha}}{\beta}\left(-i\sqrt{B} + \frac{2Gi\sqrt{B}}{G+cos\left(2\sqrt{B}\,(\xi+F)\right) + isin\left(2\sqrt{B}\,(\xi+F)\right)}\right)^{-1}, \tag{21}$$

$$V_{17,18}(x,\ y,\ t) = \pm\frac{\sqrt{\beta B\alpha}}{\beta}\left(-\frac{1}{\xi+F}\right), \tag{22}$$

For Eqs. (14)–(22), $\xi=\frac{1}{\tau}\left(\left(x+\frac{1}{\Gamma\tau}\right)^{\tau}+\left(y+\frac{1}{\Gamma\tau}\right)^{\tau}-\frac{1}{2}\frac{\sqrt{2}\sqrt{B(4B+\alpha)}}{B}\left(t+\frac{1}{\Gamma\tau}\right)^{\tau}\right)$ is used for the acquired solutions.

Set 2 represents the solutions of the analyzed model obtained by applying Eqs. (7)–(11):

$$V_{19,20}(x,\ y,\ t) = \pm\frac{\sqrt{\beta B\alpha}}{\beta}\left(\frac{\sqrt{-(G^2+H^2)B} - G\sqrt{-B}\ cosh\left(2\sqrt{-B}\,(\xi+F)\right)}{G\sinh\left(2\sqrt{-B}\,(\xi+F)\right)+H}\right)^{-1}, \tag{23}$$

$$V_{21,22}(x,\ y,\ t) = \pm\frac{\sqrt{\beta B\alpha}}{\beta}\left(\frac{-\sqrt{-(G^2+H^2)B} - G\sqrt{-B}\ cosh\left(2\sqrt{-B}\,(\xi+F)\right)}{G\sinh\left(2\sqrt{-B}\,(\xi+F)\right)+H}\right)^{-1}, \tag{24}$$

$$V_{23,24}(x,\ y,\ t) = \pm\frac{\sqrt{\beta B\alpha}}{\beta}\left(\sqrt{-B} - \frac{2G\sqrt{-B}}{G+cosh\left(2\sqrt{-B}\,(\xi+F)\right) - sinh\left(2\sqrt{-B}\,(\xi+F)\right)}\right)^{-1}, \tag{25}$$

$$V_{25,26}(x,\ y,\ t) = \pm\frac{\sqrt{\beta B\alpha}}{\beta}\left(-\sqrt{-B} + \frac{2G\sqrt{-B}}{G+cosh\left(2\sqrt{-B}\,(\xi+F)\right) + sinh\left(2\sqrt{-B}\,(\xi+F)\right)}\right)^{-1}, \tag{26}$$

$$V_{27,28}(x,\ y,\ t) = \pm\frac{\sqrt{\beta B\alpha}}{\beta}\left(\frac{\sqrt{(G^2-H^2)B} - G\sqrt{B}\ cos\left(2\sqrt{B}\,(\xi+F)\right)}{G\sin\left(2\sqrt{B}\,(\xi+F)\right)+H}\right)^{-1}, \tag{27}$$

$$V_{29,30}(x,\ y,\ t) = \pm\frac{\sqrt{\beta B\alpha}}{\beta}\left(\frac{-\sqrt{(G^2-H^2)B} - G\sqrt{B}\ cos\left(2\sqrt{B}\,(\xi+F)\right)}{G\sin\left(2\sqrt{B}\,(\xi+F)\right)+H}\right)^{-1}, \tag{28}$$

$$V_{31,32}(x,\ y,\ t)\ = \pm\frac{\sqrt{\beta B\alpha}}{\beta}\left(i\sqrt{B}-\frac{2Gi\sqrt{B}}{G+cos\left(2\sqrt{B}\left(\xi+F\right)\right)-isin\left(2\sqrt{B}\left(\xi+F\right)\right)}\right)^{-1}, \tag{29}$$

$$V_{33,34}(x,\ y,\ t) = \pm\frac{\sqrt{\beta B\alpha}}{\beta}\left(-i\sqrt{B}+\frac{2Gi\sqrt{B}}{G+cos\left(2\sqrt{B}\left(\xi+F\right)\right)+isin\left(2\sqrt{B}\left(\xi+F\right)\right)}\right)^{-1}, \tag{30}$$

$$V_{35,36}(x,\ y,\ t)\ = \pm\frac{\sqrt{\beta B\alpha}}{\beta}\left(-\frac{1}{\xi+F}\right), \tag{31}$$

For Eqs. (22)–(31), $\xi=\frac{1}{\tau}\left(\left(x+\frac{1}{\Gamma\tau}\right)^{\tau}+\left(y+\frac{1}{\Gamma\tau}\right)^{\tau}+\frac{1}{2}\frac{\sqrt{2}\sqrt{B(4B+\alpha)}}{B}\left(t+\frac{1}{\Gamma\tau}\right)^{\tau}\right)$ is used for the acquired solutions.

Set 3 represents the solutions of the analyzed model obtained by applying Eqs. (7)–(11):

$$V_{37,38}(x,y,t) = \pm\frac{\sqrt{\beta B\alpha}}{B\beta}\left(\frac{\sqrt{-(G^2+H^2)B}-G\sqrt{-B}\,cosh\left(2\sqrt{-B}(\xi+F)\right)}{Gsinh\left(2\sqrt{-B}(\xi+F)\right)+H}\right) \tag{32}$$

$$V_{39,40}(x,y,t) = \pm\frac{\sqrt{\beta B\alpha}}{B\beta}\left(\frac{-\sqrt{-(G^2+H^2)B}-G\sqrt{-B}\,cosh\left(2\sqrt{-B}(\xi+F)\right)}{Gsinh\left(2\sqrt{-B}(\xi+F)\right)+H}\right) \tag{33}$$

$$V_{41,42}(x,y,t) = \pm\frac{\sqrt{\beta B\alpha}}{B\beta}\left(\sqrt{-B}-\frac{2G\sqrt{-B}}{G+cosh\left(2\sqrt{-B}(\xi+F)\right)-sinh\left(2\sqrt{-B}(\xi+F)\right)}\right) \tag{34}$$

$$V_{43,44}(x,y,t) = \pm\frac{\sqrt{\beta B\alpha}}{B\beta}\left(-\sqrt{-B}+\frac{2G\sqrt{-B}}{G+cosh\left(2\sqrt{-B}(\xi+F)\right)+sinh\left(2\sqrt{-B}(\xi+F)\right)}\right) \tag{35}$$

$$V_{45,46}(x,\ y,\ t)\ =\ \pm\frac{\sqrt{\beta B\alpha}}{B\beta}\left(\frac{\sqrt{(G^2-H^2)B}-G\sqrt{B}\ cos\left(2\sqrt{B}\left(\xi+F\right)\right)}{Gsin\left(2\sqrt{B}\left(\xi+F\right)\right)+H}\right) \tag{36}$$

$$V_{47,48}(x,\ y,\ t)\ = \pm\frac{\sqrt{\beta B\alpha}}{B\beta}\left(\frac{-\sqrt{(G^2-H^2)B}-G\sqrt{B}\ cos\left(2\sqrt{B}\left(\xi+F\right)\right)}{Gsin\left(2\sqrt{B}\left(\xi+F\right)\right)+H}\right) \tag{37}$$

$$V_{49,50}(x,y,t) = \pm\frac{\sqrt{\beta B\alpha}}{B\beta}\left(i\sqrt{B}-\frac{2Gi\sqrt{B}}{G+cos\left(2\sqrt{B}(\xi+F)\right)-isin\left(2\sqrt{B}(\xi+F)\right)}\right) \tag{38}$$

$$V_{51,52}(x,\ y,\ t)\ =\ \pm\frac{\sqrt{\beta B\alpha}}{B\beta}\left(-i\sqrt{B}+\frac{2Gi\sqrt{B}}{G+cos\left(2\sqrt{B}\left(\xi+F\right)\right)+isin\left(2\sqrt{B}\left(\xi+F\right)\right)}\right) \tag{39}$$

$$V_{53,54}(x,\ y,\ t)\ =\ \pm\frac{\sqrt{\beta B\alpha}}{B\beta}\left(-\frac{1}{\xi+F}\right) \tag{40}$$

For Eqs. (32)–(40), $\xi=\frac{1}{\tau}\left(\left(x+\frac{1}{\Gamma\tau}\right)^{\tau}+\left(y+\frac{1}{\Gamma\tau}\right)^{\tau}-\frac{1}{2}\frac{\sqrt{2}\sqrt{B(4B+\alpha)}}{B}\left(t+\frac{1}{\Gamma\tau}\right)^{\tau}\right)$ is used for the acquired solutions.

Set 4 represents the solutions of the analyzed model obtained by applying Eqs. (7)–(11):

$$V_{55,56}(x,y,t) = \pm\frac{\sqrt{\beta B\alpha}}{B\beta}\left(\frac{\sqrt{-(G^2+H^2)B}-G\sqrt{-B}\,cosh\left(2\sqrt{-B}(\xi+F)\right)}{Gsinh\left(2\sqrt{-B}(\xi+F)\right)+H}\right) \tag{41}$$

$$V_{57,58}(x,y,t) = \pm\frac{\sqrt{\beta B\alpha}}{B\beta}\left(\frac{-\sqrt{-(G^2+H^2)B}-G\sqrt{-B}\,cosh\left(2\sqrt{-B}(\xi+F)\right)}{Gsinh\left(2\sqrt{-B}(\xi+F)\right)+H}\right) \tag{42}$$

$$V_{59,60}(x,\ y,\ t)\ =\ \pm\frac{\sqrt{\beta B\alpha}}{B\beta}\left(\sqrt{-B}-\frac{2G\sqrt{-B}}{G+cosh\left(2\sqrt{-B}\left(\xi+F\right)\right)-sinh\left(2\sqrt{-B}\left(\xi+F\right)\right)}\right) \tag{43}$$

$$V_{61,62}(x,y,t) = \pm\frac{\sqrt{\beta B\alpha}}{B\beta}\left(-\sqrt{-B}+\frac{2G\sqrt{-B}}{G+cosh\left(2\sqrt{-B}(\xi+F)\right)+sinh\left(2\sqrt{-B}(\xi+F)\right)}\right) \tag{44}$$

$$V_{63,64}(x,\ y,\ t)\ =\ \pm\frac{\sqrt{\beta B\alpha}}{B\beta}\left(\frac{\sqrt{(G^2-H^2)B}-G\sqrt{B}\ cos\left(2\sqrt{B}\left(\xi+F\right)\right)}{Gsin\left(2\sqrt{B}\left(\xi+F\right)\right)+H}\right) \tag{45}$$

$$V_{65,66}(x,\ y,\ t)\ = \pm\frac{\sqrt{\beta B\alpha}}{B\beta}\left(\frac{-\sqrt{(G^2-H^2)B}-G\sqrt{B}\ cos\left(2\sqrt{B}\left(\xi+F\right)\right)}{Gsin\left(2\sqrt{B}\left(\xi+F\right)\right)+H}\right) \tag{46}$$

$$V_{67,68}(x,y,t)=\pm\frac{\sqrt{\beta B\alpha}}{B\beta}\left(i\sqrt{B}-\frac{2Gi\sqrt{B}}{G+cos\left(2\sqrt{B}(\xi+F)\right)-isin\left(2\sqrt{B}(\xi+F)\right)}\right) \tag{47}$$

$$V_{69,70}(x,\ y,\ t)\ =\ \pm\frac{\sqrt{\beta B\alpha}}{B\beta}\left(-i\sqrt{B}+\frac{2Gi\sqrt{B}}{G+cos\left(2\sqrt{B}\,(\xi+F)\right)+isin\left(2\sqrt{B}\,(\xi+F)\right)}\right) \tag{48}$$

$$V_{71,72}(x,\ y,\ t)\ =\ \pm\frac{\sqrt{\beta B\alpha}}{B\beta}\left(-\frac{1}{\xi+F}\right) \tag{49}$$

For Eqs. (41)–(49), $\xi=\frac{1}{\tau}\left(\left(x+\frac{1}{\Gamma\tau}\right)^{\tau}+\left(y+\frac{1}{\Gamma\tau}\right)^{\tau}+\frac{1}{2}\ \frac{\sqrt{2}\ \sqrt{B(4B+\alpha)}}{B}\left(t+\frac{1}{\Gamma\tau}\right)^{\tau}\right)$ is used for the acquired solutions.

Set 5 represents the solutions of the analyzed model obtained by applying Eqs. (7)–(11):

$$\begin{aligned}V_{73,74}(x,\ y,\ t)\ =\ &\pm\left(\frac{1}{2}\frac{\sqrt{-2\beta B\alpha}}{B\beta}\left(\frac{\sqrt{-(G^2+H^2)B}-G\sqrt{-B}\ cosh\left(2\sqrt{-B}\,(\xi+F)\right)}{Gsinh\left(2\sqrt{-B}\,(\xi+F)\right)+H}\right)\right.\\&\left.-\frac{\alpha\beta}{\sqrt{-2\beta B\alpha}}\left(\frac{\sqrt{-(G^2+H^2)B}-G\sqrt{-B}\ cosh\left(2\sqrt{-B}\,(\xi+F)\right)}{Gsinh\left(2\sqrt{-B}\,(\xi+F)\right)+H}\right)^{-1}\right),\end{aligned} \tag{50}$$

$$\begin{aligned}V_{75,76}(x,\ y,\ t)\ =\ &\pm\left(\frac{1}{2}\frac{\sqrt{-2\beta B\alpha}}{B\beta}\left(\frac{-\sqrt{-(G^2+H^2)B}-G\sqrt{-B}\ cosh\left(2\sqrt{-B}(\xi+F)\right)}{Gsinh\left(2\sqrt{-B}(\xi+F)\right)+H}\right)\right.\\&\left.-\frac{\alpha\beta}{\sqrt{-2\beta B\alpha}}\left(\frac{-\sqrt{-(G^2+H^2)B}-G\sqrt{-B}\ cosh\left(2\sqrt{-B}(\xi+F)\right)}{Gsinh\left(2\sqrt{-B}(\xi+F)\right)+H}\right)^{-1}\right),\end{aligned} \tag{51}$$

$$\begin{aligned}V_{77,78}(x,\ y,\ t)\ =\ &\pm\left(\frac{1}{2}\frac{\sqrt{-2\beta B\alpha}}{B\beta}\left(\sqrt{-B}-\frac{2G\sqrt{-B}}{G+cosh\left(2\sqrt{-B}\,(\xi+F)\right)-sinh\left(2\sqrt{-B}\,(\xi+F)\right)}\right)\right.\\&\left.-\frac{\alpha\beta}{\sqrt{-2\beta B\alpha}}\left(\sqrt{-B}-\frac{2G\sqrt{-B}}{G+cosh\left(2\sqrt{-B}\,(\xi+F)\right)-sinh\left(2\sqrt{-B}\,(\xi+F)\right)}\right)^{-1}\right),\end{aligned} \tag{52}$$

$$\begin{aligned}V_{79,80}(x,\ y,\ t)\ =\ &\pm\left(\frac{1}{2}\frac{\sqrt{-2\beta B\alpha}}{B\beta}\left(-\sqrt{-B}+\frac{2G\sqrt{-B}}{G+cosh\left(2\sqrt{-B}\,(\xi+F)\right)+sinh\left(2\sqrt{-B}\,(\xi+F)\right)}\right)\right.\\&\left.-\frac{\alpha\beta}{\sqrt{-2\beta B\alpha}}\left(-\sqrt{-B}+\frac{2G\sqrt{-B}}{G+cosh\left(2\sqrt{-B}\,(\xi+F)\right)+sinh\left(2\sqrt{-B}\,(\xi+F)\right)}\right)^{-1}\right),\end{aligned} \tag{53}$$

$$\begin{aligned}V_{81,82}(x,y,t)=&\pm\left(\frac{1}{2}\frac{\sqrt{-2\beta B\alpha}}{B\beta}\left(\frac{\sqrt{(G^2-H^2)B}-G\sqrt{B}cos\left(2\sqrt{B}(\xi+F)\right)}{Gsin\left(2\sqrt{B}(\xi+F)\right)+H}\right)\right.\\&\left.-\frac{\alpha\beta}{\sqrt{-2\beta B\alpha}}\left(\frac{\sqrt{(G^2-H^2)B}-G\sqrt{B}cos\left(2\sqrt{B}(\xi+F)\right)}{Gsin\left(2\sqrt{B}(\xi+F)\right)+H}\right)^{-1}\right),\end{aligned} \tag{54}$$

$$\begin{aligned}V_{83,84}(x,y,t)=&\pm\left(\frac{1}{2}\frac{\sqrt{-2\beta B\alpha}}{B\beta}\left(\frac{-\sqrt{(G^2-H^2)B}-G\sqrt{B}cos\left(2\sqrt{B}(\xi+F)\right)}{Gsin\left(2\sqrt{B}(\xi+F)\right)+H}\right)\right.\\&\left.-\frac{\alpha\beta}{\sqrt{-2\beta B\alpha}}\left(\frac{-\sqrt{(G^2-H^2)B}-G\sqrt{B}cos\left(2\sqrt{B}(\xi+F)\right)}{Gsin\left(2\sqrt{B}(\xi+F)\right)+H}\right)^{-1}\right),\end{aligned} \tag{55}$$

$$\begin{aligned}V_{85,86}(x,\ y,\ t)\ =\ &\pm\left(\frac{1}{2}\frac{\sqrt{-2\beta B\alpha}}{B\beta}\left(i\sqrt{B}-\frac{2Gi\sqrt{B}}{G+cos\left(2\sqrt{B}\,(\xi+F)\right)-isin\left(2\sqrt{B}\,(\xi+F)\right)}\right)\right.\\&\left.-\frac{\alpha\beta}{\sqrt{-2\beta B\alpha}}\left(i\sqrt{B}-\frac{2Gi\sqrt{B}}{G+cos\left(2\sqrt{B}\,(\xi+F)\right)-isin\left(2\sqrt{B}\,(\xi+F)\right)}\right)^{-1}\right),\end{aligned} \tag{56}$$

$$\begin{aligned}V_{87,88}(x,\ y,\ t)\ =\ &\pm\left(\frac{1}{2}\frac{\sqrt{-2\beta B\alpha}}{B\beta}\left(-i\sqrt{B}+\frac{2Gi\sqrt{B}}{G+cos\left(2\sqrt{B}\,(\xi+F)\right)+isin\left(2\sqrt{B}\,(\xi+F)\right)}\right)\right.\\&\left.-\frac{\alpha\beta}{\sqrt{-2\beta B\alpha}}\left(-i\sqrt{B}+\frac{2Gi\sqrt{B}}{G+cos\left(2\sqrt{B}\,(\xi+F)\right)+isin\left(2\sqrt{B}\,(\xi+F)\right)}\right)^{-1}\right),\end{aligned} \tag{57}$$

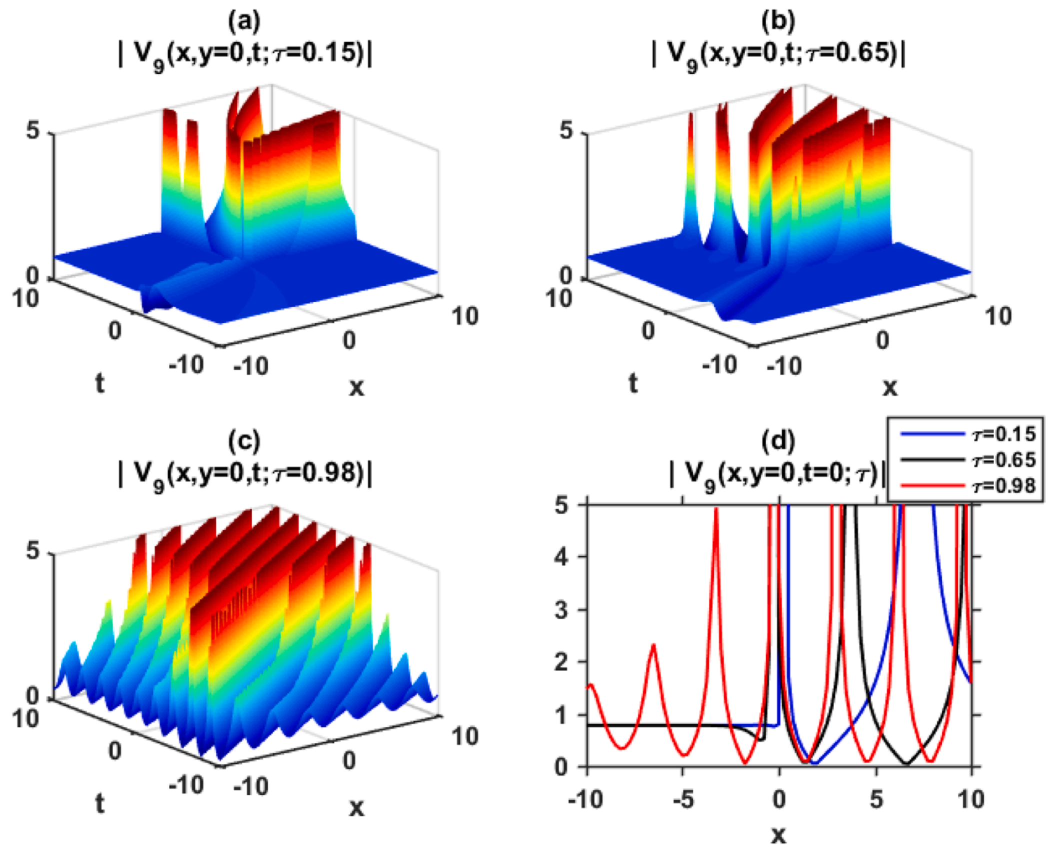

Fig. 1. Impact of the fractional parameter on the acquired solution $|V_9(x,y=0,t;\tau)|$ given by Eq. (18): (a)–(c) $\tau = 0.15, 0.65, 0.98$ for selecting particular free parameters as $\alpha = 0.3$, $\beta = 0.5$, $B = 1$, $G = 0.4$, $H = 0.25$, $F = 0$, $y = 0$, and (d) the changes in the 2D plots from (a)–(c) at time $t = 0$.

$$V_{89,90}(x,y,t)=\pm\left(\frac{1}{2}\frac{\sqrt{-2\beta B\alpha}}{B\beta}\left(-\frac{1}{\xi+F}\right)-\frac{\alpha\beta}{\sqrt{-2\beta B\alpha}}\left(-\frac{1}{\xi+F}\right)^{-1}\right), \tag{58}$$

For Eqs. (50)–(58), $\xi=\frac{1}{\tau}\left(\left(x+\frac{1}{\Gamma\tau}\right)^{\tau}+\left(y+\frac{1}{\Gamma\tau}\right)^{\tau}-\frac{1}{2}\frac{\sqrt{(8B-\alpha)B}}{B}\left(t+\frac{1}{\Gamma\tau}\right)^{\tau}\right)$ is used for the acquired solutions.

Set 6 represents the solutions of the analyzed model obtained by applying Eqs. (7)–(11):

$$\begin{aligned}V_{91,92}(x,\ y,\ t)\ =\ &\pm\left(\frac{1}{2}\frac{\sqrt{-2\beta B\alpha}}{B\beta}\left(\frac{\sqrt{-(G^2+H^2)B}-G\sqrt{-B}\,cosh\left(2\sqrt{-B}\,(\xi+F)\right)}{Gsinh\left(2\sqrt{-B}\,(\xi+F)\right)+H}\right)\right.\\&\left.-\frac{\alpha\beta}{\sqrt{-2\beta B\alpha}}\left(\frac{\sqrt{-(G^2+H^2)B}-G\sqrt{-B}\,cosh\left(2\sqrt{-B}\,(\xi+F)\right)}{Gsinh\left(2\sqrt{-B}\,(\xi+F)\right)+H}\right)^{-1}\right),\end{aligned} \tag{59}$$

$$\begin{aligned}V_{93,94}(x,\ y,\ t)\ =\ &\pm\left(\frac{1}{2}\frac{\sqrt{-2\beta B\alpha}}{B\beta}\left(\frac{-\sqrt{-(G^2+H^2)B}-G\sqrt{-B}\,cosh\left(2\sqrt{-B}\,(\xi+F)\right)}{Gsinh\left(2\sqrt{-B}\,(\xi+F)\right)+H}\right)\right.\\&\left.-\frac{\alpha\beta}{\sqrt{-2\beta B\alpha}}\left(\frac{-\sqrt{-(G^2+H^2)B}-G\sqrt{-B}\,cosh\left(2\sqrt{-B}\,(\xi+F)\right)}{Gsinh\left(2\sqrt{-B}\,(\xi+F)\right)+H}\right)^{-1}\right),\end{aligned} \tag{60}$$

$$\begin{aligned}V_{95,96}(x,\ y,\ t)\ =\ &\pm\left(\frac{1}{2}\frac{\sqrt{-2\beta B\alpha}}{B\beta}\left(\sqrt{-B}-\frac{2G\sqrt{-B}}{G+cosh\left(2\sqrt{-B}\,(\xi+F)\right)-sinh\left(2\sqrt{-B}\,(\xi+F)\right)}\right)\right.\\&\left.-\frac{\alpha\beta}{\sqrt{-2\beta B\alpha}}\left(\sqrt{-B}-\frac{2G\sqrt{-B}}{G+cosh\left(2\sqrt{-B}\,(\xi+F)\right)-sinh\left(2\sqrt{-B}\,(\xi+F)\right)}\right)^{-1}\right),\end{aligned} \tag{61}$$

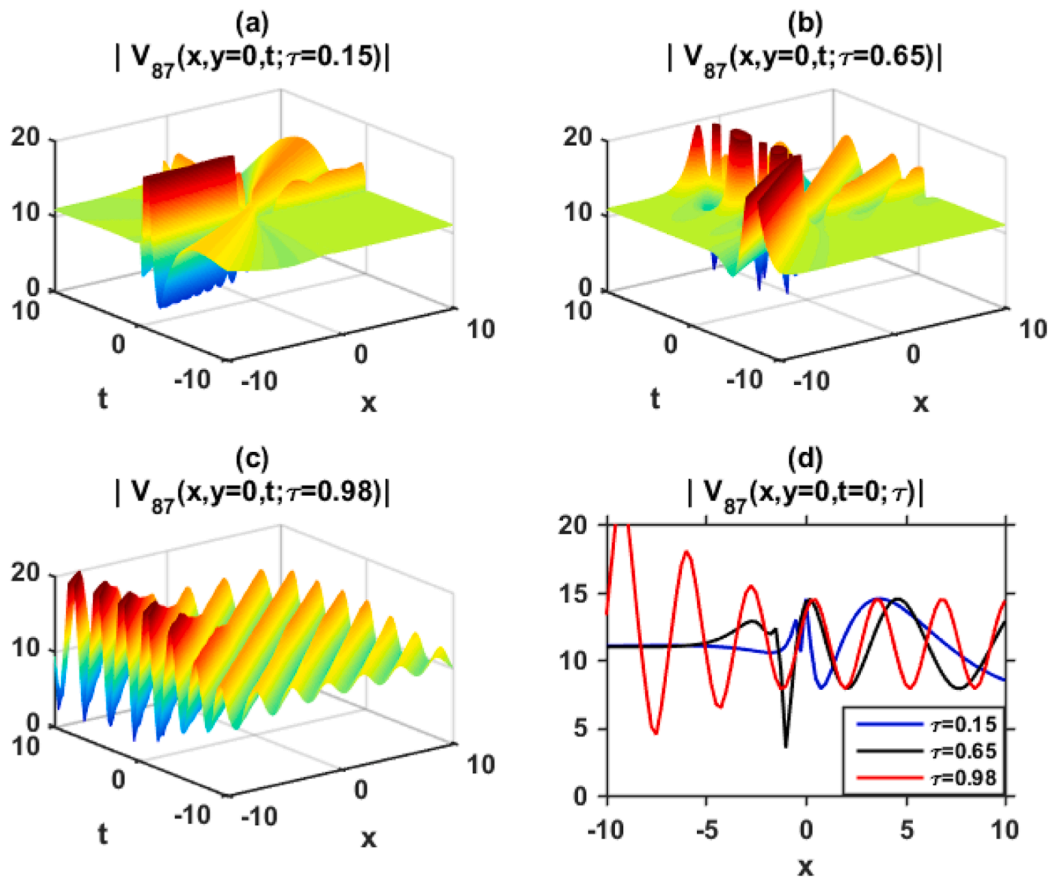

Fig. 2. Impact of the fractional parameter on the acquired solution $|V_{87}(x,y=0,t;\tau)|$ given by Eq. (57): (a)–(c) $\tau = 0.15, 0.65, 0.98$ for selecting particular free parameters as $\alpha = 3$, $\beta = 5$, $B = 1$, $G = -0.1$, $H = 3$, $F = 5$, $y = 0$, and (d) the changes in the 2D plots from (a)–(c) at time $t = 0$.

$$V_{97,98}(x,y,t)=\pm\left(\frac{1}{2}\frac{\sqrt{-2\beta B\alpha}}{B\beta}\left(-\sqrt{-B}+\frac{2G\sqrt{-B}}{G+cosh\left(2\sqrt{-B}(\xi+F)\right)+sinh\left(2\sqrt{-B}(\xi+F)\right)}\right)-\frac{\alpha\beta}{\sqrt{-2\beta B\alpha}}\left(-\sqrt{-B}+\frac{2G\sqrt{-B}}{G+cosh\left(2\sqrt{-B}(\xi+F)\right)+sinh\left(2\sqrt{-B}(\xi+F)\right)}\right)^{-1}\right), \tag{62}$$

$$V_{99,100}(x,y,t)=\pm\left(\frac{1}{2}\frac{\sqrt{-2\beta B\alpha}}{B\beta}\left(\frac{\sqrt{(G^2-H^2)B}-G\sqrt{B}cos\left(2\sqrt{B}(\xi+F)\right)}{G\sin\left(2\sqrt{B}(\xi+F)\right)+H}\right)-\frac{\alpha\beta}{\sqrt{-2\beta B\alpha}}\left(\frac{\sqrt{(G^2-H^2)B}-G\sqrt{B}cos\left(2\sqrt{B}(\xi+F)\right)}{G\sin\left(2\sqrt{B}(\xi+F)\right)+H}\right)^{-1}\right), \tag{63}$$

$$V_{101,102}(x,y,t)=\pm\left(\frac{1}{2}\frac{\sqrt{-2\beta B\alpha}}{B\beta}\left(\frac{-\sqrt{(G^2-H^2)B}-G\sqrt{B}cos\left(2\sqrt{B}(\xi+F)\right)}{G\sin\left(2\sqrt{B}(\xi+F)\right)+H}\right)-\frac{\alpha\beta}{\sqrt{-2\beta B\alpha}}\left(\frac{-\sqrt{(G^2-H^2)B}-G\sqrt{B}cos\left(2\sqrt{B}(\xi+F)\right)}{G\sin\left(2\sqrt{B}(\xi+F)\right)+H}\right)^{-1}\right), \tag{64}$$

$$V_{103,104}(x,\ y,\ t)=\pm\left(\frac{1}{2}\frac{\sqrt{-2\beta B\alpha}}{B\beta}\left(i\sqrt{B}-\frac{2Gi\sqrt{B}}{G+cos\left(2\sqrt{B}\,(\xi+F)\right)-isin\left(2\sqrt{B}\,(\xi+F)\right)}\right)-\frac{\alpha\beta}{\sqrt{-2\beta B\alpha}}\left(i\sqrt{B}-\frac{2Gi\sqrt{B}}{G+cos\left(2\sqrt{B}\,(\xi+F)\right)-isin\left(2\sqrt{B}\,(\xi+F)\right)}\right)^{-1}\right), \tag{65}$$

$$V_{105,106}(x,\ y,\ t)=\pm\left(\frac{1}{2}\frac{\sqrt{-2\beta B\alpha}}{B\beta}\left(-i\sqrt{B}+\frac{2Gi\sqrt{B}}{G+cos\left(2\sqrt{B}\,(\xi+F)\right)+isin\left(2\sqrt{B}\,(\xi+F)\right)}\right)-\frac{\alpha\beta}{\sqrt{-2\beta B\alpha}}\left(-i\sqrt{B}+\frac{2Gi\sqrt{B}}{G+cos\left(2\sqrt{B}\,(\xi+F)\right)+isin\left(2\sqrt{B}\,(\xi+F)\right)}\right)^{-1}\right), \tag{66}$$

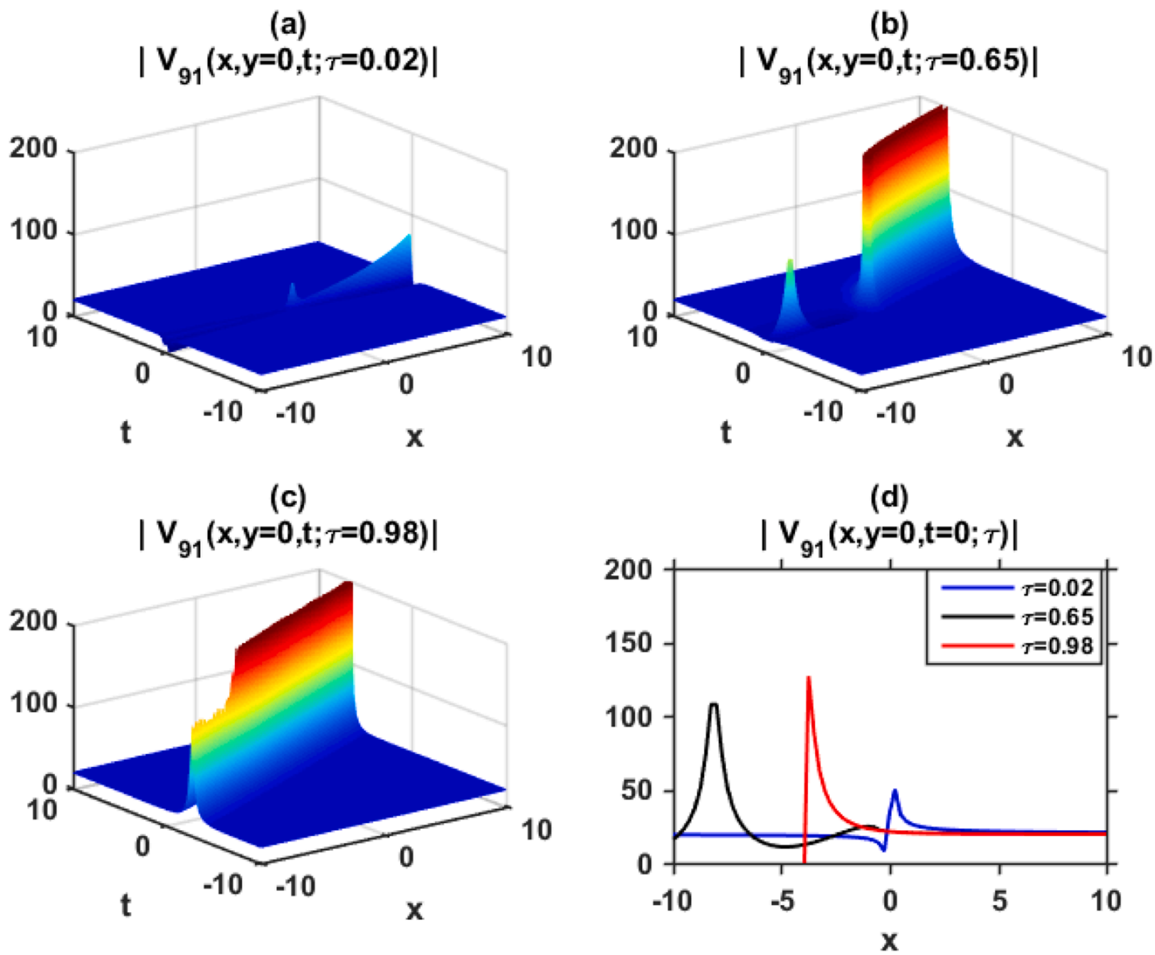

Fig. 3. Impact of the fractional parameter on the acquired solution $|V_{91}(x, y = 0, t; \tau)|$ given by Eq. (59): (a)–(c) $\tau = 0.02, 0.65, 0.98$ for selecting particular free parameters as $\alpha = 1$, $\beta = 4$, $B = -0.1$, $G = 5$, $H = 3$, $F = 5$, $y = 0$, and (d) the changes in the 2D plots from (a)–(c) at time $t = 0$.

$$V_{107,108}(x,y,t) = \pm\left(\frac{1}{2}\frac{\sqrt{-2\beta B\alpha}}{B\beta}\left(-\frac{1}{\xi+F}\right) - \frac{\alpha\beta}{\sqrt{-2\beta B\alpha}}\left(-\frac{1}{\xi+F}\right)^{-1}\right), \quad (67)$$

For Eqs. (59)–(67), $\xi = \frac{1}{\tau}\left(\left(x+\frac{1}{\Gamma\tau}\right)^{\tau} + \left(y+\frac{1}{\Gamma\tau}\right)^{\tau} + \frac{1}{2}\frac{\sqrt{(8B-\alpha)B}}{B}\left(t+\frac{1}{\Gamma\tau}\right)^{\tau}\right)$

is used for the acquired solutions.

Set 7 represents the solutions of the analyzed model obtained by applying Eqs. (7)–(11):

$$\begin{aligned} V_{109,110}(x,\ y,\ t) &= \pm\left(\frac{1}{2}\frac{\sqrt{\beta B\alpha}}{B\beta}\left(\frac{\sqrt{-(G^2+H^2)B} - G\sqrt{-B}\cosh\left(2\sqrt{-B}\,(\xi+F)\right)}{G\sinh\left(2\sqrt{-B}\,(\xi+F)\right)+H}\right)\right. \\ &\left.-\frac{1}{2}\frac{\alpha\beta}{\sqrt{\beta B\alpha}}\left(\frac{\sqrt{-(G^2+H^2)B} - G\sqrt{-B}\cosh\left(2\sqrt{-B}\,(\xi+F)\right)}{G\sinh\left(2\sqrt{-B}\,(\xi+F)\right)+H}\right)^{-1}\right), \end{aligned} \quad (68)$$

$$\begin{aligned} V_{111,112}(x,\ y,\ t) &= \pm\left(\frac{1}{2}\frac{\sqrt{\beta B\alpha}}{B\beta}\left(\frac{-\sqrt{-(G^2+H^2)B} - G\sqrt{-B}\cosh\left(2\sqrt{-B}\,(\xi+F)\right)}{G\sinh\left(2\sqrt{-B}\,(\xi+F)\right)+H}\right)\right. \\ &\left.-\frac{1}{2}\frac{\alpha\beta}{\sqrt{\beta B\alpha}}\left(\frac{-\sqrt{-(G^2+H^2)B} - G\sqrt{-B}\cosh\left(2\sqrt{-B}\,(\xi+F)\right)}{G\sinh\left(2\sqrt{-B}\,(\xi+F)\right)+H}\right)^{-1}\right), \end{aligned} \quad (69)$$

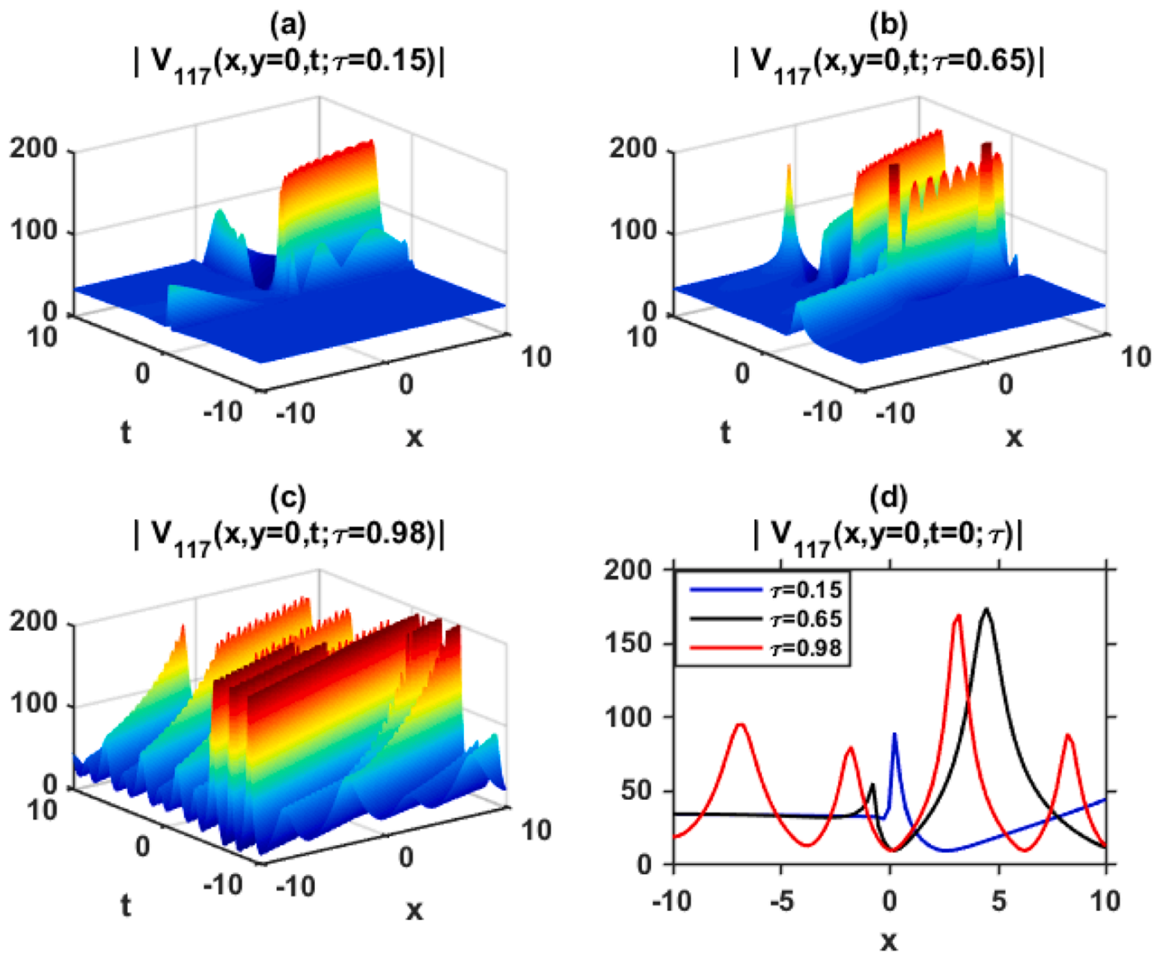

Fig. 4. Impact of the fractional parameter on the acquired solution $|V_{117}(x, y = 0, t; \tau)|$ given by Eq. (72): (a)–(c) $\tau = 0.15, 0.65, 0.98$ for selecting particular free parameters as $\alpha = 4$, $\beta = 5$, $B = 0.1$, $G = -2.9$, $H = 3$, $F = 5$, $y = 0$, and (d) the changes in the 2D plots from (a)–(c) at time $t = 0$.

$$V_{113,114}(x,\ y,\ t) = \pm\left(\frac{1}{2}\frac{\sqrt{\beta B\alpha}}{B\beta}\left(\sqrt{-B}-\frac{2G\sqrt{-B}}{G+\cosh\left(2\sqrt{-B}\,(\xi+F)\right)-\sinh\left(2\sqrt{-B}\,(\xi+F)\right)}\right) -\frac{1}{2}\frac{\alpha\beta}{\sqrt{\beta B\alpha}}\left(\sqrt{-B}-\frac{2G\sqrt{-B}}{G+\cosh\left(2\sqrt{-B}\,(\xi+F)\right)-\sinh\left(2\sqrt{-B}\,(\xi+F)\right)}\right)^{-1}\right), \tag{70}$$

$$V_{115,116}(x,\ y,\ t) = \pm\left(\frac{1}{2}\frac{\sqrt{\beta B\alpha}}{B\beta}\left(-\sqrt{-B}+\frac{2G\sqrt{-B}}{G+\cosh\left(2\sqrt{-B}\,(\xi+F)\right)+\sinh\left(2\sqrt{-B}\,(\xi+F)\right)}\right) -\frac{1}{2}\frac{\alpha\beta}{\sqrt{\beta B\alpha}}\left(-\sqrt{-B}+\frac{2G\sqrt{-B}}{G+\cosh\left(2\sqrt{-B}\,(\xi+F)\right)+\sinh\left(2\sqrt{-B}\,(\xi+F)\right)}\right)^{-1}\right), \tag{71}$$

$$V_{117,118}(x,y,t) = \pm\left(\frac{1}{2}\frac{\sqrt{\beta B\alpha}}{B\beta}\left(\frac{\sqrt{(G^2-H^2)B}-G\sqrt{B}\cos\left(2\sqrt{B}(\xi+F)\right)}{G\sin\left(2\sqrt{B}(\xi+F)\right)+H}\right) -\frac{1}{2}\frac{\alpha\beta}{\sqrt{\beta B\alpha}}\left(\frac{\sqrt{(G^2-H^2)B}-G\sqrt{B}\cos\left(2\sqrt{B}(\xi+F)\right)}{G\sin\left(2\sqrt{B}(\xi+F)\right)+H}\right)^{-1}\right), \tag{72}$$

$$V_{119,120}(x,y,t) = \pm\left(\frac{1}{2}\frac{\sqrt{\beta B\alpha}}{B\beta}\left(\frac{-\sqrt{(G^2-H^2)B}-G\sqrt{B}\cos\left(2\sqrt{B}(\xi+F)\right)}{G\sin\left(2\sqrt{B}(\xi+F)\right)+H}\right) -\frac{1}{2}\frac{\alpha\beta}{\sqrt{\beta B\alpha}}\left(\frac{-\sqrt{(G^2-H^2)B}-G\sqrt{B}\cos\left(2\sqrt{B}(\xi+F)\right)}{G\sin\left(2\sqrt{B}(\xi+F)\right)+H}\right)^{-1}\right), \tag{73}$$

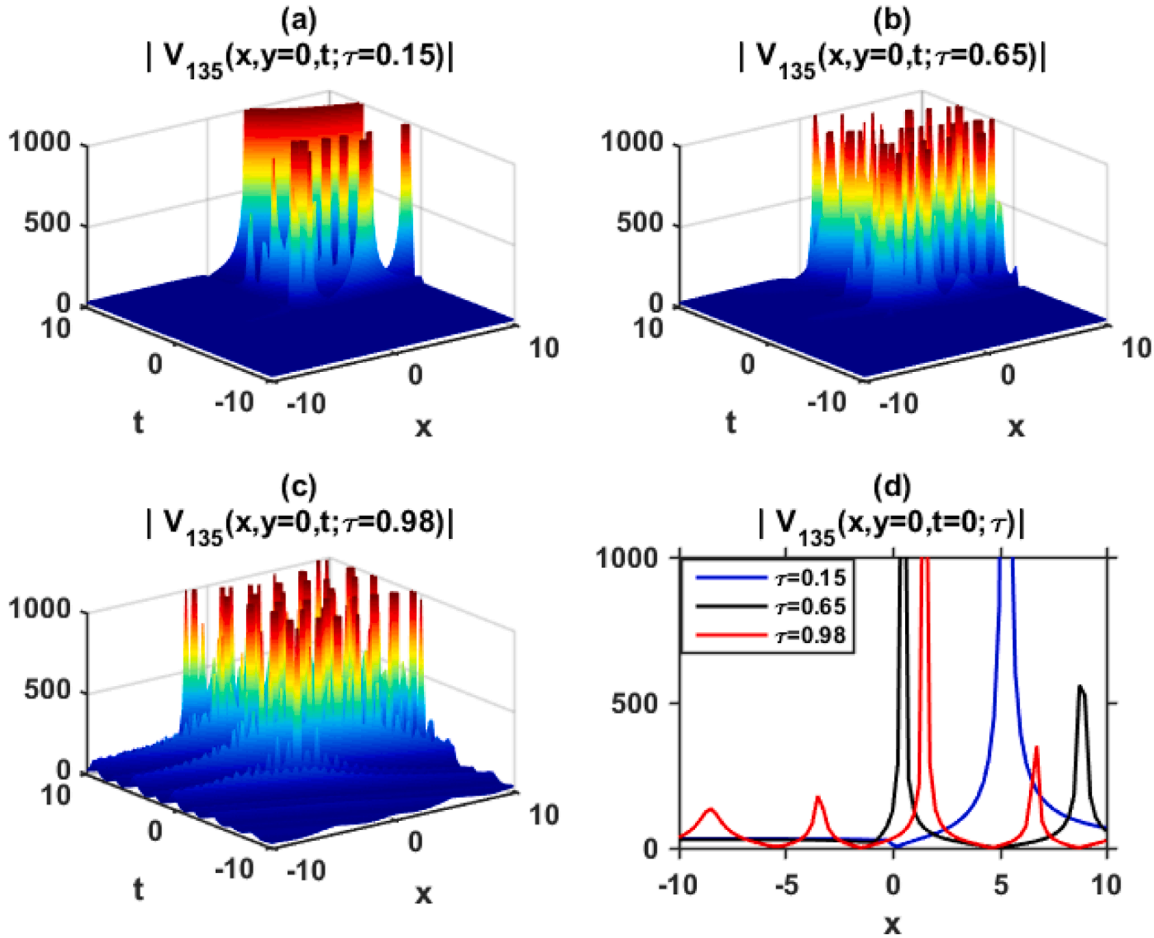

Fig. 5. Impact of the fractional parameter on the acquired solution $|V_{135}(x,y=0,t;\tau)|$ given by Eq. (81): (a)–(c) $\tau = 0.15, 0.65, 0.98$ for selecting particular free parameters as $\alpha = 3$, $\beta = 5$, $B = 0.1$, $G = 5$, $H = 3$, $F = 5$, $y = 0$, and (d) the changes in the 2D plots from (a)–(c) at time $t = 0$.

$$V_{121,122}(x,\ y,\ t) = \pm\left(\frac{1}{2}\frac{\sqrt{\beta B\alpha}}{B\beta}\left(i\sqrt{B}-\frac{2Gi\sqrt{B}}{G+cos\left(2\sqrt{B}\left(\xi+F\right)\right)-isin\left(2\sqrt{B}\left(\xi+F\right)\right)}\right)\right.$$
$$\left.-\frac{1}{2}\frac{\alpha\beta}{\sqrt{\beta B\alpha}}\left(i\sqrt{B}-\frac{2Gi\sqrt{B}}{G+cos\left(2\sqrt{B}\left(\xi+F\right)\right)-isin\left(2\sqrt{B}\left(\xi+F\right)\right)}\right)^{-1}\right), \tag{74}$$

$$V_{123,124}(x,\ y,\ t) = \pm\left(\frac{1}{2}\frac{\sqrt{\beta B\alpha}}{B\beta}\left(-i\sqrt{B}+\frac{2Gi\sqrt{B}}{G+cos\left(2\sqrt{B}\left(\xi+F\right)\right)+isin\left(2\sqrt{B}\left(\xi+F\right)\right)}\right)\right.$$
$$\left.-\frac{1}{2}\frac{\alpha\beta}{\sqrt{\beta B\alpha}}\left(-i\sqrt{B}+\frac{2Gi\sqrt{B}}{G+cos\left(2\sqrt{B}\left(\xi+F\right)\right)+isin\left(2\sqrt{B}\left(\xi+F\right)\right)}\right)^{-1}\right), \tag{75}$$

$$V_{125,126}(x,\ y,\ t) = \pm\left(\frac{1}{2}\frac{\sqrt{\beta B\alpha}}{B\beta}\left(-\frac{1}{\xi+F}\right)-\frac{1}{2}\frac{\alpha\beta}{\sqrt{\beta B\alpha}}\left(-\frac{1}{\xi+F}\right)^{-1}\right), \tag{76}$$

For Eqs. (68)–(76), $\xi=\frac{1}{\tau}\left(\left(x+\frac{1}{\Gamma\tau}\right)^{\tau}+\left(y+\frac{1}{\Gamma\tau}\right)^{\tau}-\frac{1}{4}\frac{\sqrt{2}\sqrt{(16B+\alpha)B}}{B}\left(t+\frac{1}{\Gamma\tau}\right)^{\tau}\right)$ is used for the acquired solutions.

Set 8 represents the solutions of the analyzed model obtained by applying Eqs. (7)–(11):

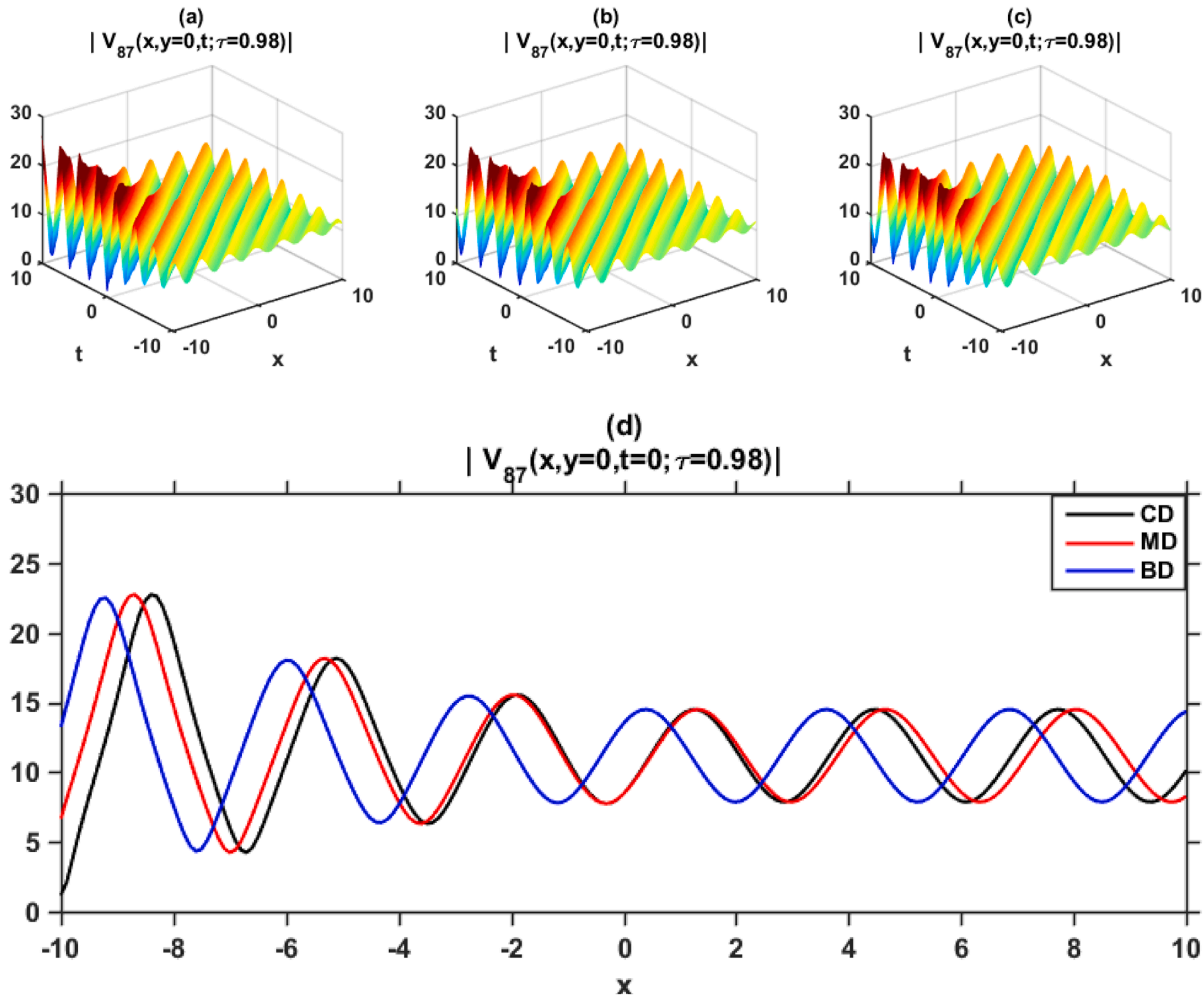

Fig. 6. The impact of the fractional parameter on the solution$|V_{87}(x,y=0,\ t=0;\ \tau=0.98)|$ as described by Eq. (86): is illustrated through 3D plots for different fractional derivatives (a) conformable derivative at $\tau=0.98$, (b) M-truncated derivative at $\tau=0.98$ and $\delta=0.9$, (c) beta derivative at $\tau=0.98$. Additionally, (d) provides a 2D waveform comparison of (a)–(c), utilizing the particular free parameters $\alpha=3$, $\beta=5$, $B=1$, $G=-0.1$, $H=3$, $F=5$, $y=0$.

$$V_{127,128}(x,\ y,\ t) = \pm\left(\frac{1}{2}\frac{\sqrt{\beta B\alpha}}{B\beta}\left(\frac{\sqrt{-(G^2+H^2)B}-G\sqrt{-B}\ cosh\left(2\sqrt{-B}\,(\xi+F)\right)}{G\sinh\left(2\sqrt{-B}\,(\xi+F)\right)+H}\right)\right.$$
$$\left.-\frac{1}{2}\frac{\alpha\beta}{\sqrt{\beta B\alpha}}\left(\frac{\sqrt{-(G^2+H^2)B}-G\sqrt{-B}\ cosh\left(2\sqrt{-B}\,(\xi+F)\right)}{G\sinh\left(2\sqrt{-B}\,(\xi+F)\right)+H}\right)^{-1}\right), \tag{77}$$

$$V_{129,130}(x,\ y,\ t) = \pm\left(\frac{1}{2}\frac{\sqrt{\beta B\alpha}}{B\beta}\left(\frac{-\sqrt{-(G^2+H^2)B}-G\sqrt{-B}\ cosh\left(2\sqrt{-B}\,(\xi+F)\right)}{G\sinh\left(2\sqrt{-B}\,(\xi+F)\right)+H}\right)\right.$$
$$\left.-\frac{1}{2}\frac{\alpha\beta}{\sqrt{\beta B\alpha}}\left(\frac{-\sqrt{-(G^2+H^2)B}-G\sqrt{-B}\ cosh\left(2\sqrt{-B}\,(\xi+F)\right)}{G\sinh\left(2\sqrt{-B}\,(\xi+F)\right)+H}\right)^{-1}\right), \tag{78}$$

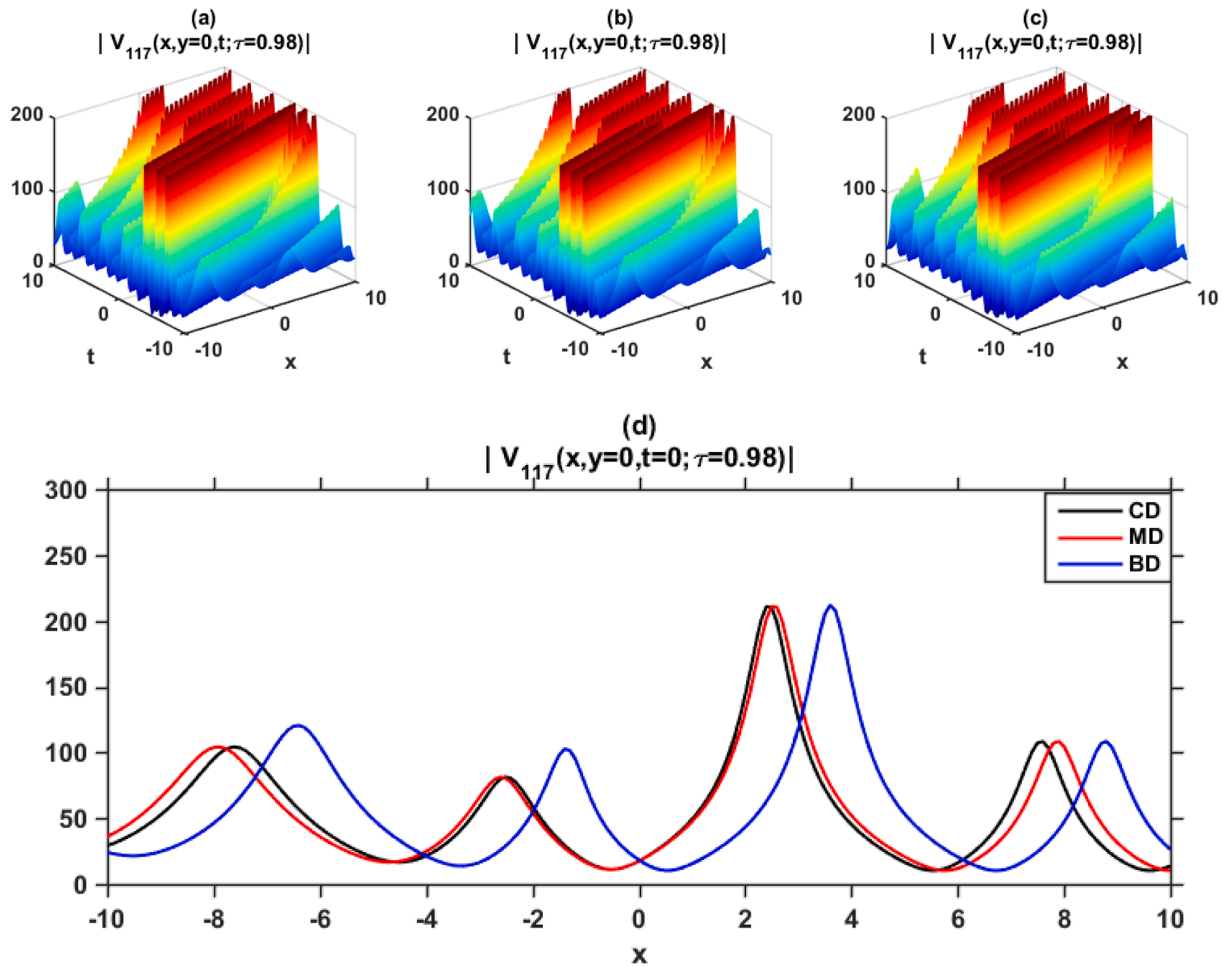

Fig. 7. The impact of the fractional parameter on the solution $|V_{117}(x,y=0,t=0;\tau=0.98)|$ as described by Eq. (87): is illustrated through 3D plots for different fractional derivatives (a) conformable derivative at $\tau=0.98$, (b) M-truncated derivative at $\tau=0.98$ and $\delta=0.9$, (c) beta derivative at $\tau=0.98$. Additionally, (d) provides a 2D waveform comparison of (a)–(c), utilizing the particular free parameters $\alpha=6$, $\beta=5$, $B=0.1$, $G=-2.9$, $H=3$, $F=5$, $y=0$.

$$V_{131,132}(x,\ y,\ t) = \pm\left(\frac{1}{2}\frac{\sqrt{\beta B\alpha}}{B\beta}\left(\sqrt{-B}-\frac{2G\sqrt{-B}}{G+cosh\left(2\sqrt{-B}\,(\xi+F)\right)-sinh\left(2\sqrt{-B}\,(\xi+F)\right)}\right)\right.$$
$$\left.-\frac{1}{2}\frac{\alpha\beta}{\sqrt{\beta B\alpha}}\left(\sqrt{-B}-\frac{2G\sqrt{-B}}{G+cosh\left(2\sqrt{-B}\,(\xi+F)\right)-sinh\left(2\sqrt{-B}\,(\xi+F)\right)}\right)^{-1}\right), \tag{79}$$

$$V_{133,134}(x,\ y,\ t) = \pm\left(\frac{1}{2}\frac{\sqrt{\beta B\alpha}}{B\beta}\left(-\sqrt{-B}+\frac{2G\sqrt{-B}}{G+cosh\left(2\sqrt{-B}\,(\xi+F)\right)+sinh\left(2\sqrt{-B}\,(\xi+F)\right)}\right)\right.$$
$$\left.-\frac{1}{2}\frac{\alpha\beta}{\sqrt{\beta B\alpha}}\left(-\sqrt{-B}+\frac{2G\sqrt{-B}}{G+cosh\left(2\sqrt{-B}\,(\xi+F)\right)+sinh\left(2\sqrt{-B}\,(\xi+F)\right)}\right)^{-1}\right), \tag{80}$$

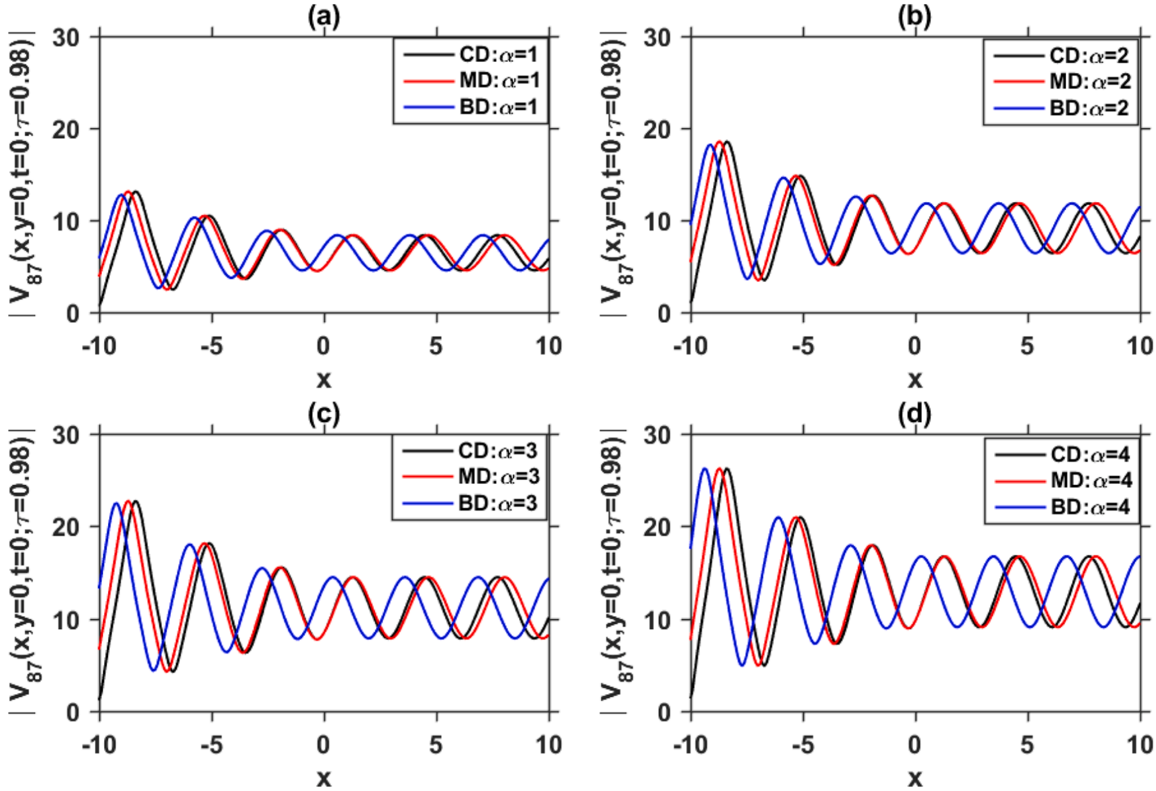

Fig. 8. Impacts of the free parameters on the cKG equation with conformable derivative at $\tau = 0.98$, M-truncated derivative at $\tau = 0.98$ and $\delta = 0.9$, beta derivative at $\tau = 0.98$ for the obtained solution given by $|V_{87}(x,y = 0, t = 0; \tau = 0.98)|$: (a)–(d) Variation of $\alpha = 1, 2, 3, 4$ when $\beta = 5$, $B = 1$, $G = -0.1$, $H = 3$, $F = 5$, $y = 0$.

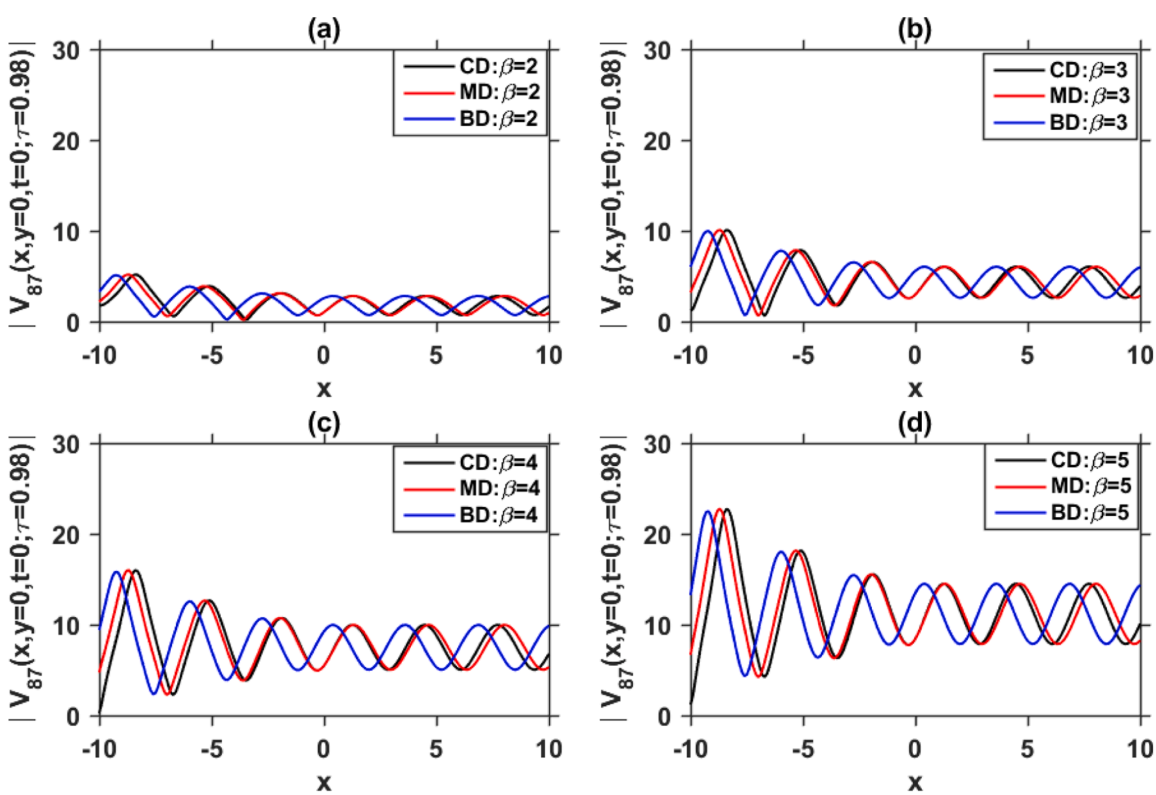

Fig. 9. Impacts of the free parameters on the cKG equation with conformable derivative at $\tau = 0.98$, M-truncated derivative at $\tau = 0.98$ and $\delta = 0.9$, beta derivative at $\tau = 0.98$ for the obtained solution given by $|V_{87}(x,y = 0, t = 0; \tau = 0.98)|$: (a)–(d) Variation of $\beta = 2, 3, 4, 5$ when $\alpha = 3$, $B = 1$, $G = -0.1$, $H = 3$, $F = 5$, $y = 0$.

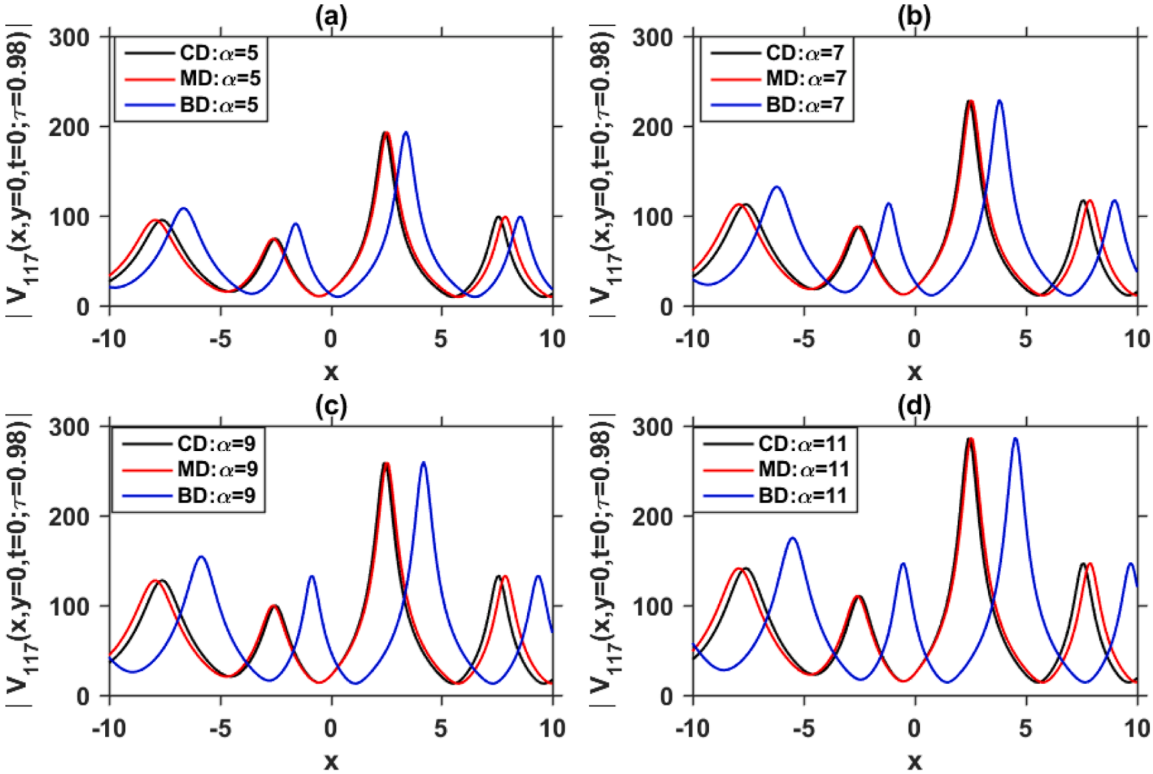

Fig. 10. Impacts of the free parameters on the cKG equation with conformable derivative at $\tau = 0.98$, M-truncated derivative at $\tau = 0.98$ and $\delta = 0.9$, beta derivative at $\tau = 0.98$ for the obtained solution given by $|V_{117}(x, y = 0, t = 0; \tau = 0.98)|$: (a)–(d) Variation of $\alpha = 5, 7, 9, 11$ when $\beta = 5$, $B = 0.1$, $G = -2.9$, $H = 3$, $F = 5$, $y = 0$.

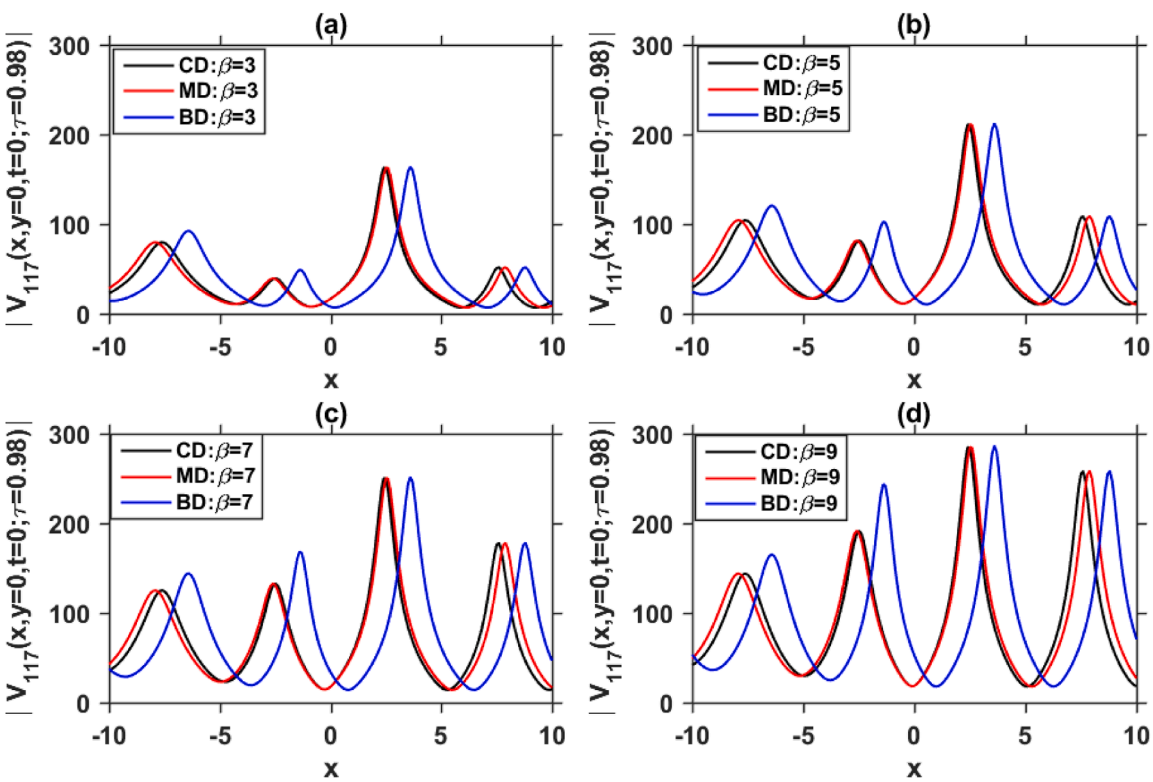

Fig. 11. Impacts of the free parameters on the cKG equation with conformable derivative at $\tau = 0.98$, M-truncated derivative at $\tau = 0.98$ and $\delta = 0.9$, beta derivative at $\tau = 0.98$ for the obtained solution given by $|V_{117}(x, y = 0, t = 0; \tau = 0.98)|$: (a)–(d) Variation of $\beta = 3, 5, 7, 9$ when $\alpha = 6$, $B = 0.1$, $G = -2.9$, $H = 3$, $F = 5$, $y = 0$.

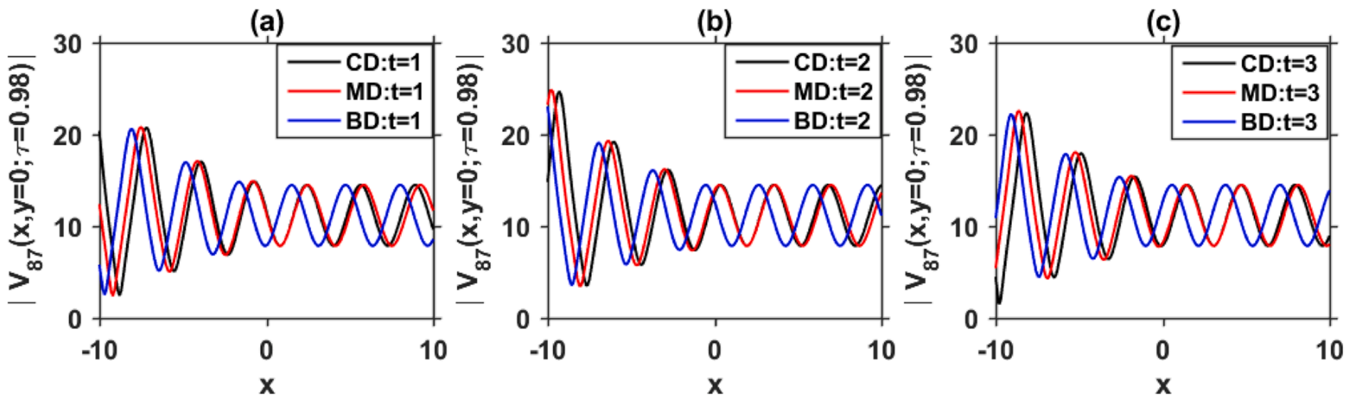

Fig. 12. Impacts of the propagation nature on the cKG equation with conformable derivative at $\tau = 0.98$, M-truncated derivative at $\tau = 0.98$ and $\delta = 0.9$, beta derivative at $\tau = 0.98$ for the obtained solution given by $|V_{87}(x, y, t; \tau = 0.98)|$: (a)–(c) $t = 1, 2, 3$ for selecting particular free parameters as $\alpha = 3, \beta = 5, B = 1, G = -0.1, H = 3, F = 5, y = 0$.

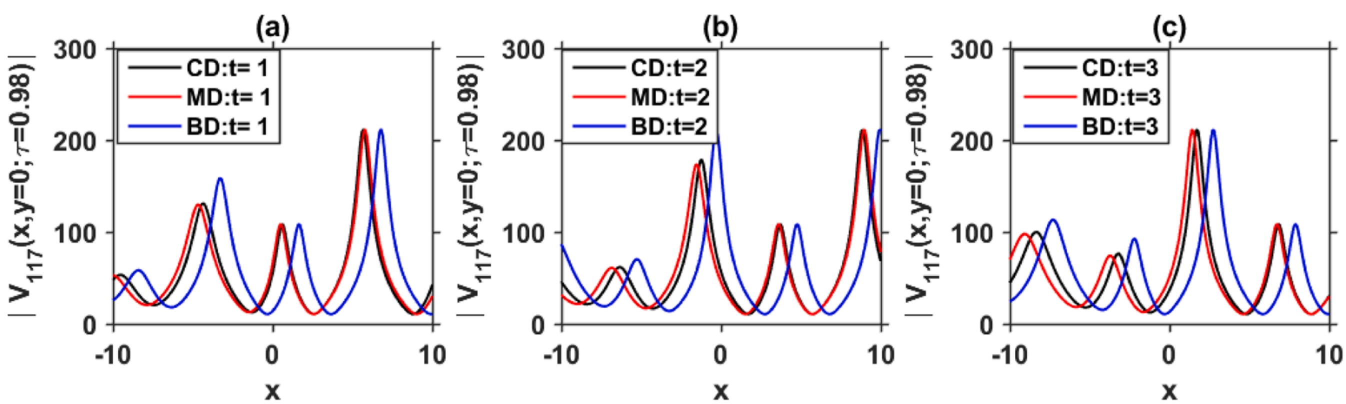

Fig. 13. Impacts of the propagation nature on the cKG equation with conformable derivative at $\tau = 0.98$, M-truncated derivative at $\tau = 0.98$ and $\delta = 0.9$, beta derivative at $\tau = 0.98$ for the obtained solution given by $|V_{117}(x, y, t; \tau = 0.98)|$: (a)–(c) $t = 1, 2, 3$ for selecting particular free parameters as $\alpha = 6, \beta = 5, B = 0.1, G = -2.9, H = 3, F = 5, y = 0$.

$$V_{135,136}(x,y,t) = \pm\left(\frac{1}{2}\frac{\sqrt{\beta B\alpha}}{B\beta}\left(\frac{\sqrt{(G^2-H^2)B}-G\sqrt{B}\cos\left(2\sqrt{B}(\xi+F)\right)}{G\sin\left(2\sqrt{B}(\xi+F)\right)+H}\right) - \frac{1}{2}\frac{\alpha\beta}{\sqrt{\beta B\alpha}}\left(\frac{\sqrt{(G^2-H^2)B}-G\sqrt{B}\cos\left(2\sqrt{B}(\xi+F)\right)}{G\sin\left(2\sqrt{B}(\xi+F)\right)+H}\right)^{-1}\right), \tag{81}$$

$$V_{137,138}(x,y,t) = \pm\left(\frac{1}{2}\frac{\sqrt{\beta B\alpha}}{B\beta}\left(\frac{-\sqrt{(G^2-H^2)B}-G\sqrt{B}\cos\left(2\sqrt{B}(\xi+F)\right)}{G\sin\left(2\sqrt{B}(\xi+F)\right)+H}\right) - \frac{1}{2}\frac{\alpha\beta}{\sqrt{\beta B\alpha}}\left(\frac{-\sqrt{(G^2-H^2)B}-G\sqrt{B}\cos\left(2\sqrt{B}(\xi+F)\right)}{G\sin\left(2\sqrt{B}(\xi+F)\right)+H}\right)^{-1}\right), \tag{82}$$

$$V_{139,140}(x,\ y,\ t) = \pm\left(\frac{1}{2}\frac{\sqrt{\beta B\alpha}}{B\beta}\left(i\sqrt{B} - \frac{2Gi\sqrt{B}}{G+\cos\left(2\sqrt{B}(\xi+F)\right) - i\sin\left(2\sqrt{B}(\xi+F)\right)}\right) - \frac{1}{2}\frac{\alpha\beta}{\sqrt{\beta B\alpha}}\left(i\sqrt{B} - \frac{2Gi\sqrt{B}}{G+\cos\left(2\sqrt{B}(\xi+F)\right) - i\sin\left(2\sqrt{B}(\xi+F)\right)}\right)^{-1}\right), \tag{83}$$

$$V_{141,142}(x,\ y,\ t) = \pm\left(\frac{1}{2}\frac{\sqrt{\beta B\alpha}}{B\beta}\left(-i\sqrt{B} + \frac{2Gi\sqrt{B}}{G+\cos\left(2\sqrt{B}(\xi+F)\right) + i\sin\left(2\sqrt{B}(\xi+F)\right)}\right) - \frac{1}{2}\frac{\alpha\beta}{\sqrt{\beta B\alpha}}\left(-i\sqrt{B} + \frac{2Gi\sqrt{B}}{G+\cos\left(2\sqrt{B}(\xi+F)\right) + i\sin\left(2\sqrt{B}(\xi+F)\right)}\right)^{-1}\right), \tag{84}$$

$$V_{143,144}(x,y,t)=\pm\left(\frac{1}{2}\frac{\sqrt{\beta B\alpha}}{B\beta}\left(-\frac{1}{\xi+F}\right)-\frac{1}{2}\frac{\alpha\beta}{\sqrt{\beta B\alpha}}\left(-\frac{1}{\xi+F}\right)^{-1}\right), \tag{85}$$

For Eqs. (77)–(85), $\xi=\frac{1}{\tau}\left(\left(x+\frac{1}{\Gamma\tau}\right)^{\tau}+\left(y+\frac{1}{\Gamma\tau}\right)^{\tau}+\frac{1}{4}\frac{\sqrt{2}\sqrt{(16B+\alpha)B}}{B}\left(t+\frac{1}{\Gamma\tau}\right)^{\tau}\right)$ is used for the acquired solutions. It is important to note that the derived hyperbolic function solutions are valid for $B<0$, while the trigonometric function solutions apply when $B>0$.

Physical interpretation of the derived solutions

This section will address the physical representation of the obtained exact solutions for the (2+1)-dimensional cubic Klein–Gordon equation. A graphical representation of the physical characteristics of the obtained solutions, as depicted in Figs. 1–5, was utilized to plot all the derived solutions. These represent periodic, periodic with equal wavelength, bright, periodic with unequal wavelength, periodic singular with unequal wavelength and other soliton solutions, respectively. The unified method produces soliton solutions with fractional characteristics for the fractional-order cKG equation. To demonstrate the impact of the fractional parameter on the obtained solutions $|V_9(x,y=0,t;\tau)|$, $|V_{87}(x,y=0,t;\tau)|$, $|V_{91}(x,y=0,t;\tau)|$, $|V_{117}(x,y=0,t;\tau)|$, and $|V_{135}(x,y=0,t;\tau)|$ provided by Eq. (18), Eq. (57), Eq. (59), Eq. (72) and Eq. (81). Fig. 1**(a)–(c),** Fig. 2**(a)–(c),** Fig. 4**(a)–(c), and** Fig. 5**(a)–(c)** present 3D graphs under different fractional values ($\tau=0.15, 0.65, 0.98$), respectively. Fig. 3**(a)–(c)** present 3D graphs under different fractional values ($\tau=0.02, 0.65, 0.98$). Fig. 1, the selected free parameters are $\alpha=0.3$, $\beta=0.5$, $B=1$, $G=0.4$, $H=0.25$, $F=0$ for solution $|V_9(x,y=0,t;\tau)|$. Fig. 2, the selected free parameters are $\alpha=3$, $\beta=5$, $B=1$, $G=-0.1$, $H=3$, $F=5$ for solution $|V_{87}(x,y=0,t;\tau)|$. Fig. 3, the selected free parameters are $\alpha=1$, $\beta=4$, $B=-0.1$, $G=5$, $H=3$, $F=5$ for solution $|V_{91}(x,y=0,t;\tau)|$. Fig. 4, the selected free parameters are $\alpha=4$, $\beta=5$, $B=0.1$, $G=-2.9$, $H=3$, $F=5$ for solution $|V_{117}(x,y=0,t;\tau)|$. Fig. 5, the selected free parameters are $\alpha=3$, $\beta=5$, $B=0.1$, $G=5$, $H=3$, $F=5$ for solution $|V_{135}(x,y=0,t;\tau)|$. The 2D plots along the x-axis at $t=0$ for the mentioned solutions are depicted in Fig. 1**(d),** Fig. 2**(d),** Fig. 4**(d), and** Fig. 5**(d),** respectively, under different fractional values ($\tau=0.15, 0.65, 0.98$). The 2D plots along the x-axis at $t=0$ for the mentioned solutions are depicted in Fig. 3**(d)** under different fractional values ($\tau=0.02, 0.65, 0.98$). The number of oscillations of the periodic wave increases with the increase of fractional parameters, as shown in Figs. 1**(d),** 2**(d),** 4**(d), and** 5**(d).** It is found, however, that the amplitudes of the wave profiles change toward the x-axis but are nearly identical for the different values of $\tau=0.15$, 0.65 and 0.98. Fig. 3**(d)** shows that the amplitudes slightly increase as the fractional parameter rises. Furthermore, the profile fully develops into a bright soliton when τ is set to 0.98.

A comparative analysis of the beta derivative in relation to other fractional derivatives

In this research, we carried out a comparative analysis of the beta derivative, a type of fractional derivative, against other fractional derivatives. A fractional PDE can be transformed into an ODE using these derivatives, which makes analysis easier. The conformable derivative, the M-truncated derivative, and the beta derivative are the three differential fractional derivatives on which we emphasize. Depending on the specific conditions, the variable $V(x,y,t)$ can be transformed into $v(\xi)$ through various transformations:for the conformable derivative, $\xi=\frac{1}{\tau}(x^{\tau}+y^{\tau}-\lambda t^{\tau})$; for the M-truncated derivative, $\xi=\frac{\Gamma(\delta+1)}{\tau}(x^{\tau}+y^{\tau}-\lambda t^{\tau})$; and for the beta derivative, $\xi=\frac{1}{\tau}\left(\left(x+\frac{1}{\Gamma\tau}\right)^{\tau}+\left(y+\frac{1}{\Gamma\tau}\right)^{\tau}-\lambda\left(t+\frac{1}{\Gamma\tau}\right)^{\tau}\right)$. These transformations are used to reduce the fractional PDE in Eq. (10) to an ODE, as shown in Eq. (12). Evaluating and contrasting the transformed variables in a comparative study requires careful consideration of their significant relationship with the fractional parameter. This section explores two solutions by examining the conformable derivative, the M-truncated derivative, and the beta derivative, to assess the effectiveness of the study's derivative results compared to those obtained using the unified method. The solutions presented in Eqs. (57) and (72) are expressed using the conformable derivative, M-truncated derivative, and beta derivative:

$$\begin{aligned}V_{87}(x,y,t)=&\pm\left(\frac{1}{2}\frac{\sqrt{-2\beta B\alpha}}{B\beta}\left(-i\sqrt{B}+\frac{2Gi\sqrt{B}}{G+cos\left(2\sqrt{B}(\xi+F)\right)+isin\left(2\sqrt{B}(\xi+F)\right)}\right)\right.\\&\left.-\frac{\alpha\beta}{\sqrt{-2\beta B\alpha}}\left(-i\sqrt{B}+\frac{2Gi\sqrt{B}}{G+cos\left(2\sqrt{B}(\xi+F)\right)+isin\left(2\sqrt{B}(\xi+F)\right)}\right)^{-1}\right)\end{aligned} \tag{86}$$

where for the conformable derivative, $\xi=\frac{1}{\tau}\left(x^{\tau}+y^{\tau}-\frac{1}{2}\frac{\sqrt{(8B-\alpha)B}}{B}t^{\tau}\right)$ is employed, for the M-truncated derivative, $\xi=\frac{\Gamma(\delta+1)}{\tau}\left(x^{\tau}+y^{\tau}-\frac{1}{2}\frac{\sqrt{(8B-\alpha)B}}{B}t^{\tau}\right)$ is used, whereas for the beta derivative, $\xi=\frac{1}{\tau}\left(\left(x+\frac{1}{\Gamma\tau}\right)^{\tau}+\left(y+\frac{1}{\Gamma\tau}\right)^{\tau}-\frac{1}{2}\frac{\sqrt{(8B-\alpha)B}}{B}\left(t+\frac{1}{\Gamma\tau}\right)^{\tau}\right)$ is used.

$$\begin{aligned}V_{117}(x,y,t)=&\pm\left(\frac{1}{2}\frac{\sqrt{\beta B\alpha}}{B\beta}\left(\frac{\sqrt{(G^2-H^2)B}-G\sqrt{B}\cos\left(2\sqrt{B}(\xi+F)\right)}{G\sin\left(2\sqrt{B}(\xi+F)\right)+H}\right)\right.\\&\left.-\frac{1}{2}\frac{\alpha\beta}{\sqrt{\beta B\alpha}}\left(\frac{\sqrt{(G^2-H^2)B}-G\sqrt{B}\cos\left(2\sqrt{B}(\xi+F)\right)}{G\sin\left(2\sqrt{B}(\xi+F)\right)+H}\right)^{-1}\right)\end{aligned} \tag{87}$$

where for the conformable derivative, $\xi=\frac{1}{\tau}\left(x^{\tau}+y^{\tau}-\frac{1}{4}\frac{\sqrt{2}\sqrt{(16B+\alpha)B}}{B}t^{\tau}\right)$ is employed, for the M-truncated derivative, $\xi=\frac{\Gamma(\delta+1)}{\tau}\left(x^{\tau}+y^{\tau}-\frac{1}{4}\frac{\sqrt{2}\sqrt{(16B+\alpha)B}}{B}t^{\tau}\right)$ is used, whereas for the beta derivative, $\xi=\frac{1}{\tau}\left(\left(x+\frac{1}{\Gamma\tau}\right)^{\tau}+\left(y+\frac{1}{\Gamma\tau}\right)^{\tau}-\frac{1}{4}\frac{\sqrt{2}\sqrt{(16B+\alpha)B}}{B}\left(t+\frac{1}{\Gamma\tau}\right)^{\tau}\right)$ is used.

To confirm the validity of our analyzed solutions, Figs. 6 **and** 7 compare three fractional wave solutions, as described by Eqs. (86) and (87), in relation to the conformable derivative, M-truncated derivative, and beta derivative. The graphical representations in Figs. 6 **and** 7 clearly demonstrate the consistent patterns observed across all solution profiles for the various derivatives under consideration. The solutions obtained in this study show a remarkable consistency with those derived using beta derivative methods. After carefully examining the findings, it can be said with confidence that the solutions that were investigated and based on the conformable derivative framework show a significant level of agreement with the outcomes that were obtained using the beta derivative methodology. Fig. 6 we take $\alpha = 3$, $\beta = 5$, $B = 1$, $G = -0.1$, $H = 3$, $F = 5$, $y = 0$ in $|V_{87}(x,y = 0,\ t = 0;\ \tau = 0.98)|$ where Fig. 6**(a)–(c)** present the 3D structure for conformable derivative at $\tau = 0.98$, M-truncated derivative at $\tau = 0.98$ and $\delta = 0.9$, beta derivative at $\tau = 0.98$, and Fig. 6**(d)** present the 2D comparison between conformable derivative, M-truncated derivative, beta derivative for $\tau = 0.98$ and $\delta = 0.9$. The amplitude of solitons is the same compared to the conformable derivative, M-truncated derivative, and beta derivative with the same fractional value. The conformable derivative and the M-truncated derivative come very close to each other but the beta derivative shows different behavior. Fig. 7 we take $\alpha = 6$, $\beta = 5$, $B = 0.1$, $G = -2.9$, $H = 3$, $F = 5$, $y = 0$ in $|V_{117}(x,y = 0,\ t = 0;\ \tau = 0.98)|$ where Figs. 7**(a)**, 7**(c)** present the 3D structure for conformable derivative at $\tau = 0.98$, M-truncated derivative at $\tau = 0.98$ and $\delta = 0.9$, beta derivative at $\tau = 0.98$, and Fig. 7**(d)** present the 2D comparison between conformable derivative, M-truncated derivative, beta derivative for $\tau = 0.98$ and $\delta = 0.9$. Similar tendencies have been discovered for Fig. 7**.** A similar observation on the behavior of each of the periodic, bright, periodic singular with unequal wavelength and other type solitons are found, but the sake of brevity, they are overlooked.

Results and discussion

Impacts of free parameters

Figs. 8**(a)–**8**(d),** 9**(a)–**9**(d),** 10**(a)–**10**(d),** and 11**(a)–**11**(d)** illustrate the impacts of the free parameters α and β on periodic solitons with equal and unequal wavelength within the cKG model equation, using the conformable derivative at $\tau = 0.98$, the M-truncated derivative at $\tau = 0.98$ with $\delta = 0.9$, and the beta derivative at $\tau = 0.98$.The soliton outlines along the x-axis vary with different values of the free parameter $\alpha = 1, 2, 3, 4$, and $\alpha = 5, 7, 9, 11$, as demonstrated in Figs. 8**(a)–(d)** and 10 **(a)–(d).** Figs. 8**(a)–**8**(d)** and 10**(a)–**10**(d)** show that, while the other parameters stay unchanged, the amplitude increases as the values of α increase. The fixed parameter values in Fig. 8**(a)–**8**(d)** are $\beta = 5$, $B = 1$, $G = -0.1$, $H = 3$, $F = 5$. The fixed parameter values in Fig. 10**(a)–**10**(d)** are $\beta = 5$, $B = 0.1$, $G = -2.9$, $H = 3$, $F = 5$. Similar patterns have been observed for the values of $\beta = 2, 3, 4, 5$ and $\beta = 3, 5, 7, 9$ which are shown in Fig. 9**(a)–**9**(d)** and Fig. 11**(a)–**11**(d),** respectively. The remaining parameters are also fixed in this case. $\alpha = 3$, $B = 1$, $G = -0.1$, $H = 3$, and $F = 5$ are the fixed parameter values in Fig. 9**(a)–(d).** $\alpha = 6$, $B = 0.1$, $G = -2.9$, $H = 3$, and $F = 5$ are the fixed parameter values in **11 (a)-11(d).** Here, increasing the values of the free parameters in the context of conformable derivative, M-truncated derivative and beta derivative leads to changes in the amplitude. The solutions change uniformly in the same manner altogether.

Wave propagation behaviors of the obtained solutions

Figs. 12**(a)–**12**(c) and** 13**(a)–**13**(c)** depict the wave propagation behaviors of periodic with equal and unequal wavelength solitons in the cKG model equation using the conformable derivative at $\tau = 0.98$, the M-truncated derivative at $\tau = 0.98$ with $\delta = 0.9$, and the beta derivative at $\tau = 0.98$. The periodic soliton solution $|V_{87}(x,y,\ t;\ \tau = 0.98)|$ is depicted in Fig. 12 along with its propagation behavior for a sequence of times t = 1, 2, 3. As the value of time (t) rises, the location of the periodic soliton shifts, as observed in Fig. 12**(a)–**12**(c).** With increasing time, the soliton is propagating from the x-axis negative side to its positive side. The fixed parameter values in Fig. 12**(a)–(c)** are $\alpha = 3$, $\beta = 5$, $B = 1$, $G = -0.1$, $H = 3$, $F = 5$, $y = 0$. For a sequence of times$t = 1, 2, 3$ the propagation characteristic of the periodic unequal wavelength soliton solution $|V_{91}(x,y,\ t;\ \tau = 0.98)|$ is illustrated in Fig. 13. According to Fig. 13 **(a)–(c)**, the soliton's position changes as time (t) increases. As time increases, the soliton propagates from the negative side of the x-axis towards the positive side. Fig. 13**(a)–(c),** the fixed parameter values are $\alpha = 6$, $\beta = 5$, $B = 0.1$, $G = -2.9$, $H = 3$, $F = 5$, $y = 0$.

Conclusions

In this study, the unified method with beta derivative is applied to the (2+1)-dimensional cKG equation to find some novel soliton solutions. Here, we provide the main findings of the research. The unified method generates various soliton solutions, including periodic, periodic with equal wavelength, bright, periodic with unequal wavelength, and periodic singular with unequal wavelength, incorporating the beta derivative, as presented in Figs. 1–5. The conformable derivative, M-truncated derivative, and beta derivative are compared in Figs. 7 and 8. Figs. 8–11 display the 2D plots and physical descriptions of the conformable derivative, M-truncated derivative, and beta derivative for comparison. Additionally, Figs. 8–11 show how the free parameters(α, β) affected the examined periodic solitons with equal and unequal wavelength. It has been found that the soliton profiles vary with changes in the free parameters. Figs. 12 and 13 provide a graphic explanation of the obtained solutions wave propagation patterns.The summarized findings show that the solitons using the beta derivative exhibit distinct behavior when $\alpha = 0.98$, unlike the conformable derivative and M-truncated derivative, which displayed similar shapes and structures. Another important point to note here is that the given solitons can also be used to explain the wave propagation characteristics in physical and communication systems. As a result, the solutions discovered could assist researchers in future studies to better understand the unidentified wave advancing in the field of communication systems.

Compliance with ethical standards

This article does not contain any studies with human or animal subjects.

CRediT authorship contribution statement

K. M. Abdul Al Woadud: Conceptualization, Methodology, Formal analysis, Software, Validation, Writing - original draft. **Md. Jahirul Islam**: Resources, Writing - review editing. **Dipankar Kumar**: Conceptualization, Formal analysis, Data curation, Resources, Software, Validation, Supervision, Writing - review editing. **Aminur Rahman Khan**: Formal analysis, Resources, Supervision, Writing - review editing.

Declaration of competing interest

The authors declare that they have no known competing financial interests or personal relationships that could have appeared to influence the work reported in this paper.

Acknowledgment

The authors are grateful to the editor and two anonymous referees for their careful reading of our manuscript and their insightful comments and useful suggestions that helped us to improve the article.

Data availability

Data will be made available on request.

References

1. Khan K, Akbar MA. Exact solutions of the (2+ 1)-dimensional cubic Klein–Gordon equation and the (3+ 1)-dimensional Zakharov–Kuznetsov equation using the modified simple equation method. *J Assoc Arab Univ Basic Appl Sci*. 2014;15:74–81. Apr 1.
2. Ozkan A., Ozkan E.M. Exact solutions of the space time-fractional Klein–Gordon equation with cubic nonlinearities using some methods. arXiv preprint arXiv: 2006.00832. 2020 Jun 1.
3. Wang M, Zhou Y, Li Z. Application of a homogeneous balance method to exact solutions of nonlinear equations in mathematical physics. *Phys Lett A*. 1996;216(1-5):67–75. Jun 17.
4. Hossain AK, Akbar MA, Azad MA. Closed form wave solutions of two nonlinear evolution equations. *Cogent Phys*. 2017;4(1), 1396948. Jan 1.
5. Fan E. Extended tanh-function method and its applications to nonlinear equations. *Phys Lett A*. 2000;277(4-5):212–218. Dec 4.
6. Abdou MA. The extended F-expansion method and its application for a class of nonlinear evolution equations. *Chaos Solitons Fractals*. 2007;31(1):95–104. Jan 1.
7. Zayed EM, Gepreel KA. The (G′/G)-expansion method for finding traveling wave solutions of nonlinear partial differential equations in mathematical physics. *J Math Phys*. 2009;50(1). Jan 1.
8. Khater MM, Kumar D. New exact solutions for the time fractional coupled Boussinesq–Burger equation and approximate long water wave equation in shallow water. *J Ocean Eng Sci*. 2017;2(3):223–228. Sep 1.
9. Chen Y, Yan Z. The Weierstrass elliptic function expansion method and its applications in nonlinear wave equations. *Chaos Solitons Fractals*. 2006;29(4): 948–964. Aug 1.
10. Ma WX, Lee JH. A transformed rational function method and exact solutions to the 3 + 1 dimensional Jimbo–Miwa equation. *Chaos Solitons Fractals*. 2009;42(3): 1356–1363. Nov 15.
11. Chen Y, Yan Z. The Weierstrass elliptic function expansion method and its applications in nonlinear wave equations. *Chaos Solitons Fractals*. 2006;29(4): 948–964. Aug 1.
12. Hosseini K, Samadani F, Kumar D, Faridi M. New optical solitons of cubic-quartic nonlinear Schrödinger equation. *Optik*. 2018;157:1101–1105. Mar 1.
13. Kumar D, Seadawy AR, Joardar AK. Modified Kudryashov method via new exact solutions for some conformable fractional differential equations arising in mathematical biology. *Chin J Phys*. 2018;56(1):75–85. Feb 1.
14. Kumar D, Darvishi MT, Joardar AK. Modified Kudryashov method and its application to the fractional version of the variety of Boussinesq-like equations in shallow water. *Opt Quantum Electron*. 2018;50:1–7. Mar.
15. Joardar AK, Kumar D, Al Woadud KA. New exact solutions of the combined and double combined sinh-cosh-Gordon equations via modified Kudryashov method. *Int J Phys Res*. 2018;1:25–30.
16. Al Woadud KA, Kumar D, Islam MJ, ImrulKayes M, Joardar AK. Analytic solutions of the chiral nonlinear schrödinger equations investigated by an efficient approach. *Int J Phys Res*. 2019;7:94–99.
17. Al Woadud KA, Kumar D, Islam MJ, Kayes MI, Kundu AK. Extraction of solitary wave features to the Heisenberg ferromagnetic spin chain and the complex Klein–Gordon equations. *Int J Appl Comput Math*. 2019;5:1. Jun.
18. Kumar D, Hosseini K, Samadani F. The sine-Gordon expansion method to look for the traveling wave solutions of the Tzitzéica type equations in nonlinear optics. *Optik*. 2017;149:439–446. Nov 1.
19. Kumar D, Seadawy AR, Chowdhury R. On new complex soliton structures of the nonlinear partial differential equation describing the pulse narrowing nonlinear transmission lines. *Opt Quantum Electron*. 2018;50:1–4. Feb.
20. Kumar D, Manafian J, Hawlader F, Ranjbaran A. New closed form soliton and other solutions of the Kundu–Eckhaus equation via the extended sinh-Gordon equation expansion method. *Optik*. 2018;160:159–167. May 1.
21. Foroutan M, Kumar D, Manafian J, Hoque A. New explicit soliton and other solutions for the conformable fractional Biswas–Milovic equation with Kerr and parabolic nonlinearity through an integration scheme. *Optik*. 2018;170:190–202. Oct 1.
22. Seadawy AR, Kumar D, Chakrabarty AK. Dispersive optical soliton solutions for the hyperbolic and cubic-quintic nonlinear Schrödinger equations via the extended sinh-Gordon equation expansion method. *Eur Phys J Plus*. 2018;133(5):182. May 1.
23. Seadawy AR, Kumar D, Hosseini K, Samadani F. The system of equations for the ion sound and Langmuir waves and its new exact solutions. *Results Phys*. 2018;9: 1631–1634. Jun 1.
24. Kumar S, Niwas M. New optical soliton solutions of Biswas–Arshed equation using the generalised exponential rational function approach and Kudryashov's simplest equation approach. *Pramana*. 2022;96(4):204. Oct 13.
25. Kumar S, Niwas M. New optical soliton solutions and a variety of dynamical wave profiles to the perturbed Chen–Lee–Liu equation in optical fibers. *Opt Quantum Electron*. 2023;55(5):418. May.
26. Kumar S, Niwas M, Dhiman SK. Abundant analytical soliton solutions and different wave profiles to the Kudryashov-Sinelshchikov equation in mathematical physics. *J Ocean Eng Sci*. 2022;7(6):565–577. Dec 1.
27. Kumar S, Niwas M, Wazwaz AM. Lie symmetry analysis, exact analytical solutions and dynamics of solitons for (2+ 1)-dimensional NNV equations. *Phys Scr*. 2020;95 (9), 095204. Jul 30.
28. Niwas M, Kumar S, Kharbanda H. Symmetry analysis, closed-form invariant solutions and dynamical wave structures of the generalized (3+ 1)-dimensional breaking soliton equation using optimal system of Lie subalgebra. *J Ocean Eng Sci*. 2022;7(2):188–201. Apr 1.
29. Kumar S, Niwas M. Exact closed-form solutions and dynamics of solitons for a (2+ 1)-dimensional universal hierarchy equation via Lie approach. *Pramana*. 2021;95 (4):195. Dec.
30. Rani S, Kumar S, Kumar R. Invariance analysis for determining the closed-form solutions, optimal system, and various wave profiles for a (2+ 1)-dimensional weakly coupled B-Type Kadomtsev-Petviashvili equations. *J Ocean Eng Sci*. 2023;8 (2):133–144. Mar 1.
31. Kumar S, Rani S. Lie symmetry reductions and dynamics of soliton solutions of (2+ 1)-dimensional Pavlov equation. *Pramana*. 2020;94(1):116. Dec.
32. Kumar S, Rani S. Study of exact analytical solutions and various wave profiles of a new extended (2+ 1)-dimensional Boussinesq equation using symmetry analysis. *J Ocean Eng Sci*. 2022;7(5):475–484. Oct 1.
33. Kumar S, Rani S. Invariance analysis, optimal system, closed-form solutions and dynamical wave structures of a (2+ 1)-dimensional dissipative long wave system. *Phys Scr*. 2021;96(12), 125202. Aug 10.
34. Kumar S, Rani S, Mann N. Diverse analytical wave solutions and dynamical behaviors of the new (2+ 1)-dimensional Sakovich equation emerging in fluid dynamics. *Eur Phys J Plus*. 2022;137(11):1226. Nov 9.
35. Rani S, Kumar S, Mann N. On the dynamics of optical soliton solutions, modulation stability, and various wave structures of a (2+ 1)-dimensional complex modified Korteweg-de-Vries equation using two integration mathematical methods. *Opt Quantum Electron*. 2023;55(8):731. Aug.
36. Mann N, Rani S, Kumar S, Kumar R. Novel closed-form analytical solutions and modulation instability spectrum induced by the Salerno equation describing nonlinear discrete electrical lattice via symbolic computation. *Math Comput Simul*. 2024;219:473–490. May 1.
37. Kaur L. Exact solutions of (2+ 1) dimensional cubic Klein–Gordon (cKG) equation. *Int J Math Eng Manag Sci*. 2022;7(5):613.
38. Khan K, Akbar MA. Exact solutions of the (2+ 1)-dimensional cubic Klein–Gordon equation and the (3+ 1)-dimensional Zakharov–Kuznetsov equation using the modified simple equation method. *J Assoc Arab Univ Basic Appl Sci*. 2014;15:74–81. Apr 1.
39. Asaduzzaman M, Kilicman A, Ali MZ, Sapar SH. Fixed point theorem based solvability of 2-Dimensional dissipative cubic nonlinear Klein–Gordon equation. *Mathematics*. 2020;8(7):1103. Jul 5.
40. Javeed S, Imran T, Ahmad H, Tchier F, Zhao YH. New soliton solutions of modified (3+ 1)-D Wazwaz–Benjamin–Bona–Mahony and (2+ 1)-D cubic Klein–Gordon equations using first integral method. *Open Phys*. 2023;21(1), 20220229. Mar 30.
41. Seadawy AR, Lu DC, Arshad M. Stability analysis of solitary wave solutions for coupled and (2+ 1)-dimensional cubic Klein–Gordon equations and their applications. *Commun Theor Phys*. 2018;69(6):676. Jun 1.
42. Gözükızıl ÖF, Akçağıl Ş, Aydemir T. Unification of all hyperbolic tangent function methods. *Open Phys*. 2016;14(1):524–541. Jan 1.
43. Akcagil S, Aydemir T. A new application of the unified method. *New Trends Math Sci*. 2018;6(1). Jan 1.
44. Malfliet W, Hereman W. The tanh method: I. Exact solutions of nonlinear evolution and wave equations. *Phys Scr*. 1996;54(6):563. Dec 1.
45. Fan E. Extended tanh-function method and its applications to nonlinear equations. *Phys Lett A*. 2000;277(4-5):212–218. Dec 4.
46. Elwakil SA, El-Labany SK, Zahran MA, Sabry R. Modified extended tanh-function method and its applications to nonlinear equations. *Appl Math Comput*. 2005;161(2): 403–412. Feb 15.
47. Khuri SA. A complex tanh-function method applied to nonlinear equations of Schrödinger type. *Chaos Solitons Fractals*. 2004;20(5):1037–1040. Jun 1.
48. Wang M, Li X, Zhang J. The (G′ G)-expansion method and travelling wave solutions of nonlinear evolution equations in mathematical physics. *Phys Lett A*. 2008;372(4): 417–423. Jan 21.
49. Zhang J, Wei X, Lu Y. A generalized (G′ G)-expansion method and its applications. *Phys Lett A*. 2008;372(20):3653–3658. May 12.
50. Nuruzzaman M, Kumar D, Paul GC. Fractional low-pass electrical transmission line model: dynamic behaviors of exact solutions with the impact of fractionality and free parameters. *Results Phys*. 2021;27, 104457. Aug 1.
51. Kumar D, Paul GC. Solitary and periodic wave solutions to the family of nonlinear conformable fractional Boussinesq-like equations. *Math Methods Appl Sci*. 2021;44 (4):3138–3158. Mar 15.
52. Bonyah E, Atangana A, Khan MA. Modeling the spread of computer virus via Caputo fractional derivative and the beta-derivative. *Asia Pac J Comput Eng*. 2017;4:1–5. Dec.
53. Ortigueira MD. Comments on "Modeling fractional stochastic systems as non-random fractional dynamics driven Brownian motions". *Appl Math Model*. 2009;33 (5):2534–2537. May 1.
54. Jumarie G. Modified Riemann-Liouville derivative and fractional Taylor series of nondifferentiable functions further results. *Comput Math Appl*. 2006;51(9-10): 1367–1376. May 1.
55. Khalil R, Al Horani M, Yousef A, Sababheh M. A new definition of fractional derivative. *J Comput Appl Math*. 2014;264:65–70. Jul 1.
56. Abdeljawad T. On conformable fractional calculus. *J Comput Appl Math*. 2015;279: 57–66. May 1.

57. İlhan E, Kıymaz İO. A generalization of truncated M-fractional derivative and applications to fractional differential equations. *Appl Math Nonlinear Sci*. 2020;5(1): 171–188. Jan.
58. Bas E, Ozarslan R. Real world applications of fractional models by Atangana–Baleanu fractional derivative. *Chaos Solitons Fractals*. 2018;116:121–125. Nov 1.
59. Khater MM, Ghanbari B, Nisar KS, Kumar D. Novel exact solutions of the fractional Bogoyavlensky–Konopelchenko equation involving the Atangana-Baleanu-Riemann derivative. *Alex Eng J*. 2020;59(5):2957–2967. Oct 1.
60. Atangana A, Baleanu D, Alsaedi A. Analysis of time-fractional Hunter-Saxton equation: a model of neumatic liquid crystal. *Open Phys*. 2016;14(1):145–149. Jan 1.
61. Atangana A, Alqahtani RT. Modelling the spread of river blindness disease via the caputo fractional derivative and the beta-derivative. *Entropy*. 2016;18(2):40. Jan 26.
62. Tarasov VE. No violation of the Leibniz rule. No fractional derivative. *Commun Nonlinear Sci Numer Simul*. 2013;18(11):2945–2948. Nov 1.
63. Cresson J, Szafrańska A. Comments on various extensions of the Riemann–Liouville fractional derivatives: about the Leibniz and chain rule properties. *Commun Nonlinear Sci Numer Simul*. 2020;82, 104903. Mar 1.
64. Teodoro GS, Machado JT, De Oliveira EC. A review of definitions of fractional derivatives and other operators. *J Comput Phys*. 2019;388:195–208. Jul 1.